Genome Medicine

RESEARCH

Open Access

Multi-omics uncovers immune-modulatory molecules in plasma contributing to resistance exercise-ameliorated locomotor disability after incomplete spinal cord injury

Ren Zhou[1†], Jibao Chen[2†], Yunhan Tang[1†], Chuijin Wei[1], Ping Yu[1], Xinmei Ding[3], Li'ao Zhu[4], Jiajia Yao[2], Zengqiang Ouyang[2], Jing Qiao[1], Shumin Xiong[1], Liaoliao Dong[1], Tong Yin[1], Haiqing Li[5*], Ye Feng[2*] and Lin Cheng[1*]

Abstract

Background Exercise rehabilitation therapy has garnered widespread recognition for its beneficial effects on the restoration of locomotor function in individuals with spinal cord injury (SCI). Notably, resistance exercise has demonstrated significant improvements in muscle strength, coordination, and overall functional recovery. However, to optimize clinical management and mimic exercise-like effects, it is imperative to obtain a comprehensive understanding of the molecular alterations that underlie these positive effects.

Methods We conducted a randomized controlled clinical trial investigating the effects of resistance exercise therapy for incomplete SCI. We integrated the analysis of plasma proteomics and peripheral blood mononuclear cells (PBMC) transcriptomics to explore the molecular and cellular changes induced by resistance exercise. Subsequently, we established a weight-loaded ladder-climbing mouse model to mimic the physiological effects of resistance exercise, and we analyzed the plasma proteome and metabolome, as well as the transcriptomes of PBMC and muscle tissue. Lastly, to confirm the transmissibility of the neuroprotective effects induced by resistance exercise, we intravenously injected plasma obtained from exercised male mice into SCI female mice during the non-acute phase.

Results Plasma proteomic and PBMC transcriptomic profiling underscored the notable involvement of the complement pathways and humoral immune response in the process of restoring locomotor function following SCI in the human trial. Moreover, it was emphasized that resistance exercise interventions could effectively modulate these pathways. Through employing plasma proteomic profiling and transcriptomic profiling of PBMC and muscle tissues in mice, our study revealed immunomodulatory responses that parallel those observed in human trials. In addition, our analysis of plasma metabolomics revealed an enhancement in lipid metabolism following resistance

[†]Ren Zhou, Jibao Chen and Yunhan Tang contributed equally to this paper.

*Correspondence:
Haiqing Li
drlihaiqing@163.com
Ye Feng
fengye0509@163.com
Lin Cheng
lincheng@shsmu.edu.cn
Full list of author information is available at the end of the article

exercise. We observed that resistance exercise plasma exhibited significant effects in ameliorating locomotor disability after SCI via reducing demyelination and inhibiting neuronal apoptosis.

Conclusions Our investigation elucidates the molecular alterations associated with resistance exercise therapy promoting recovery of locomotor function following incomplete SCI. Moreover, we demonstrate the direct neuroprotective effects delivered via exercise plasma injection, which facilitates spinal cord repair. Mechanistically, the comprehensive multi-omics analysis involving both human and mice reveals that the principal constituents responsible for the observed neuroprotective effects within the plasma are predominantly immunoregulatory factors, warranting further experimental validation.

Trial registration The study was retrospectively registered on 17 July, 2024, in Chinese Clinical Trial Registry (No.: ChiCTR2400087038) at https://www.chictr.org.cn/.

Keywords Resistance exercise, Multi-omics, Proteome, Metabolome, Spinal cord injury, Neuroprotection

Background

Over the decades, exercise has been recognized as an effective intervention for enhancing tissue functionality under normal physiological conditions and facilitating functional recovery in various pathological states, which offers novel strategies for regenerative medicine and finds extensive applications in various domains [1–3]. While the advantages of exercise in improving overall health and managing various diseases are widely recognized, the precise molecular mechanisms responsible for these exercise-associated benefits remain elusive and are currently being actively explored. Notably, it has been discovered that exercise stimulates the production of a wide range of bioactive molecules, including cytokines, growth factors, hormones, and other signaling molecules, in different tissues throughout the body [4, 5]. These molecules, collectively known as exerkines, play pivotal roles in maintaining internal homeostasis and acting as mediators of inter-organ communication, which has emerged as a novel avenue in the pursuit of tissue functional restoration [6].

Currently, physical exercise has been well-documented to offer notable benefits to the central nervous system, leading to its widespread adoption as a routine treatment for various neurological disorders, including spinal cord injury (SCI) [7–11]. SCI represents a severe neuropathological condition that often results in compromised somatic motor function, sensory perception, and autonomic regulation, potentially posing life-threatening consequences for affected individuals [12]. Compelling clinical evidence supports the notion that exercise training in individuals with chronic SCI yields significant improvements in various fitness outcomes, including enhancements in cardiorespiratory fitness, power output, and muscle strength [13–15]. It is worth noting that the majority of fitness benefits have been observed across various endurance exercise modalities, such as rowing, wheeling, and ambulation with an exoskeleton or body weight-supported treadmill [16]. Indeed, it has been widely recognized that endurance exercise benefits the nervous system by enhancing synaptic plasticity, promoting remyelination and neuronal survival, and facilitating neurovascular angiogenesis [17–19]. Moreover, the discovery of exerkines, such as brain-derived neurotrophic factor (BDNF) [20, 21], clusterin [22] and glycosylphosphatidylinositol (GPI)–specific phospholipase D1 (Gpld1) [23], that confer neuroprotective effects significantly enhances the theoretical foundation for promoting neural health through endurance exercise. Indeed, endurance exercise or gait rehabilitation often relies on specialized equipment, such as exoskeletons or treadmills, which may limit its accessibility and convenience. In contrast, resistance exercise (strength exercise) can be implemented with relative convenience and flexibility. Furthermore, considering the well-established benefits of resistance exercise in promoting muscle strength among healthy individuals, resistance exercise training has gained considerable importance in rehabilitation of paralyzed muscles following SCI [24, 25]. Recently, it has been summarized the notable increases in muscle strength, endurance, and power following resistance exercise training in chronic SCI patients [26]. However, there is limited research on whether resistance exercise can promote locomotor ability in individuals with SCI. In addition, the presence of factors in exercise-conditioned plasma that can positively affect locomotor function after SCI, as well as their potential for direct transferability, remains still uncertain.

Based on our current hypothesis, it was proposed that resistance exercise could not only improve muscle strength but also facilitate the recovery of locomotor function following SCI. Importantly, it was hypothesized that these therapeutic effects might be mediated through the release of circulating molecules. Thus, we conducted a human trial recruiting a cohort of participants with incomplete SCI. These patients were assigned randomly to two distinct resistance exercise treatment

groups: isometric resistance exercise (unchanging range of motion) and isotonic resistance exercise (unchanging force throughout a range of motion). We assessed the patients' locomotor function and evaluated systemic changes at a comprehensive level through proteomic and transcriptomic analyses. Subsequently, we established a mouse model of weight-loaded ladder-climbing exercise mimicking resistance training and further demonstrated the systemic adaptive physiological changes induced by resistance exercise across various dimensions, including plasma metabolome, plasma proteome, and peripheral blood mononuclear cells (PBMC) transcriptome. Finally, we administered plasma obtained from exercised male mice to evaluate its therapeutic potential for alleviating locomotor disabilities in female mice during the non-acute phase of SCI. Thus, our findings identified resistance exercise enhanced the muscle strength and improved locomotor ability in patients with incomplete SCI, with isotonic resistance exercise being more effective than isometric resistance exercise. Remarkably, our study provides validation that short-term resistance exercise induced molecular changes primarily associated with the activation of the humoral immune response and complement pathways in both humans and mice. Therapeutically, we observed that resistance exercise plasma markedly reduced demyelination and inhibited neuronal apoptosis following SCI, thereby ameliorating locomotor disability in mice, revealing the potential transformative value of plasma substances.

Methods

Participant recruitment

All participants were recruited from Shanghai Yangzhi Rehabilitation Hospital from April 2020 to October 2021 (Additional file 2: Fig. S1). This clinical trial has ceased recruiting participants, with the first participant enrolled in April 3rd, 2020, and the last participant enrolled in September 3rd, 2021, respectively. The study protocol was approved by the Ethics Committee of the Shanghai Yangzhi Rehabilitation Hospital (YZ-2020–019). All the participants signed the informed consent form before the trial. The study was retrospectively registered in Chinese Clinical Trial Registry (No.: ChiCTR2400087038) at https://www.chictr.org.cn/. The detailed protocol for this clinical trial is presented in an additional document (Additional file 3).

Participants were admitted to the study if they met the following criteria: (a) incomplete SCI patients aged over 18 years old with no progressive diseases (met with the 2019 International Neurological Classification of Spinal Cord Injury) [27]; (b) non-acute stage (duration of injury exceeding 3 months); (c) bilateral knee extensors strength were grade 3 or 4; (d) targeted muscles had stable innervation (muscle strength had not increased by more than 2 grades in the past 3 weeks). While patients were excluded from the study if any of the following criteria were present: (a) any obstacles to test or train targeted muscles (inability to change posture, insufficient range of knee extension or targeted lower-extremity muscular tension was rated above level 2 by the Modified Ashworth Scale); (b) inability to cooperate or tolerate training (severe cardiopulmonary dysfunction, cognitive impairment and unable to communicate); (c) smoking, concurrent systemic disease, metabolic disorders, cancers, and other neurological diseases.

Human exercise interventions

The exercise intervention comprised a 4-week period of resistance exercise training, targeting the quadriceps muscles. The participants underwent either isometric or isotonic exercises, with 3 sets per day and 3 days per week, under the guidance of a trained facilitator (Fig. 1A). Within the weekly training regimen, a structured approach to resistance exercise was adopted, with alternating exercise and rest days (e.g., training on the first, third, and fifth days). This design allowed for a period of 72 h of uninterrupted rest following 3 consecutive exercise days, prior to proceeding with the subsequent week's training plan. Such an arrangement ensured adequate recovery and adaptation between sessions, thereby optimizing the effectiveness and outcomes of the resistance exercise intervention.

The participants were randomly assigned to the isometric resistance exercise group and the isotonic resistance exercise group. Regardless of whether the training strategy was isotonic or isometric, the bilateral lower extremities underwent sequential training, with the left lower extremity trained prior to the right lower extremity. The training frequency for each leg of both groups was standardized as follows: 10 repetitions per set, a 2-min rest period between sets, 3 sets per day, and training sessions conducted 3 days per week over a total duration of 4 weeks. In detail, the participants of isometric resistance exercise group were seated with their hips flexed at an angle of 80 to 85° and their knees flexed at 90°, and they were instructed to contract the quadriceps with maximum force without any motion, as the distal legs were fixed [28]. Visual feedback was provided with air pressure stabilizer. Participants took rest for 5 s after 5 s of exertion. While the participants in the isotonic resistance exercise group were seated in the same position as those in the isometric exercise group. They were instructed to straighten their knees as much as possible, aiming for maximum extension. Prior to the subjects' initial training session, a one-repetition maximum (1RM) test was conducted, during which participants were instructed

to perform resistance exercises using a predetermined weight until exhaustion. The resistance weight and the number of repetitions achieved were duly recorded and subsequently entered into an online website (https://strengthlevel.com/one-rep-max-calculator) for calculation. The formal isotonic training commenced with a load corresponding to 60% of each participant's baseline 1RM. Following the completion of 3 sets consisting of 10 repetitions each, the weight was progressively increased by 5 to 10% for subsequent training sessions [29].

All participants received other regular rehabilitation programs, and participant's muscles could undergo strength training at the request of their therapists except for the quadriceps. The regular rehabilitation treatment consisted of managing secondary complications, learning the skills of mat exercise and personalized rehabilitation education. Based on participants' individualized rehabilitation goals, their rehabilitation protocols were designed by the whole team consisting of doctors, physical therapists, occupational therapists, social workers, and nurses.

Clinical outcome assessment

In this trail, the peak torque of the quadriceps femoris was designated as the primary clinical outcome, while parameters related to balance and walking, including 10-m walk test (10MWT), functional reach test (FRT), and 3-Meter Timed Up and Go (TUG), were classified as secondary clinical outcomes. The clinical outcome assessments were conducted on the participants at three time points: prior to the initiation of training, 48 h after the last training session in the second week and in the fourth week (typically between 8 a.m. to 10 a.m.). During the assessment process, blinded assessors, who were unaware of the participants' group allocation, performed the assessments for all participants. Participants were given strict instructions, emphasizing the importance of refraining from discussing their training or group allocation with both the assessors and other participants.

Peak torque assessment

Peak torque of the quadriceps muscle was tested using the isokinetic device (Biodex Isokinetic Dynamometer—System 4, USA). The participants were seated with 80 to 85° of hip flexion and 70° of knee flexion when testing peak torque. For the knee extension isometric contractions, participants performed 3 sets of continuous force exertion for 3 s each, with a break of 50 s between each contraction [30]. To determine the strength of each side, the mean of the three peak torques obtained from testing on that specific side was calculated. Additionally, to assess overall strength for each subject, the average of the peak torques from both sides (bilateral) was computed and considered as the outcome measure for strength.

10-m walk test

Participants positioned themselves at the starting line, which was set at 10 m. If they required walking aids, such as canes or frames, they were allowed to hold them in their hands. Participants were then instructed to walk twice along the 10-m distance at their normal walking speed. The time taken to cover the distance from the second to the eighth meter was recorded. To calculate the participant's normal walking speed, the distance covered within the 6 m (from the second to the eighth meter) was divided by the average time spent on the test. This calculated value represented the result of the 10MWT.

Functional reach test

Participants assumed either a sitting or standing position while facing a wall. With their shoulder joint flexed

(See figure on next page.)

Fig. 1 Locomotor function in response to resistance exercise, and locomotorfunction-associated proteome. **A** Workflow of the clinical trial of resistance exercise treating the patients with incomplete spinal cord injury (SCI). (Created with BioRender). **B** Bar plot showing the mean values of the clinical outcomes in response to resistance exercise treatment across the overall patients. Fold change (FC) of peak torque represents the performance of muscle strength, FC of walking speed represents performance of the 10-m walk test, FC of time represents performance in the Timed Up and Go test, and FC of reaching distance represents performance in the functional reach test. Each dot is expressed as the ratio to the mean of baseline in all samples. Data are expressed as means ± SEM. One-way repeated measures ANOVA with Dunnett's multiple comparisons test, $n = 20$. **C** Bar plots showing the mean values of the clinical outcomes in subgroups (Isometric exercise and isotonic exercise groups), respectively. Each dot is expressed as the ratio to the mean of baseline in each exercise group. Data are expressed as means ± SEM. One-way repeated measures ANOVA with Dunnett's multiple comparisons test, $n = 10$. **D** Venn diagram illustrating the overlap of proteins identified in the isometric exercise and isotonic exercise groups, and three-dimensional scatter plot showing principal component analysis (PCA) based on the overlapping proteins. Each dot represents a sample and colors represent detection time. **E** Bar plot representing the partial-correlated protein quantities of the four clinical outcomes, and Venn diagram showing the overlap of these proteins. The proteins listed within the box represent the overlapping regions of the Venn diagram, with the color of the box corresponding to the colors of the numbers displayed within the diagram. **F** Gene Ontology (GO) enrichment analysis showing key enriched terms of 21 proteins that overlap among the three locomotor function-related proteins, including biological process (BP), cellular component (CC), and molecular function (MF). The bar represents the fold enrichment factor, and the line graph indicates the count of proteins enriched by the pathway. **G–I** Chord diagram visualizing the top enriched pathways (GO: BP) associated with peak torque (**G**), walking speed (**H**), and TUG (**I**), and their Spearman's rank correlations with associated proteins

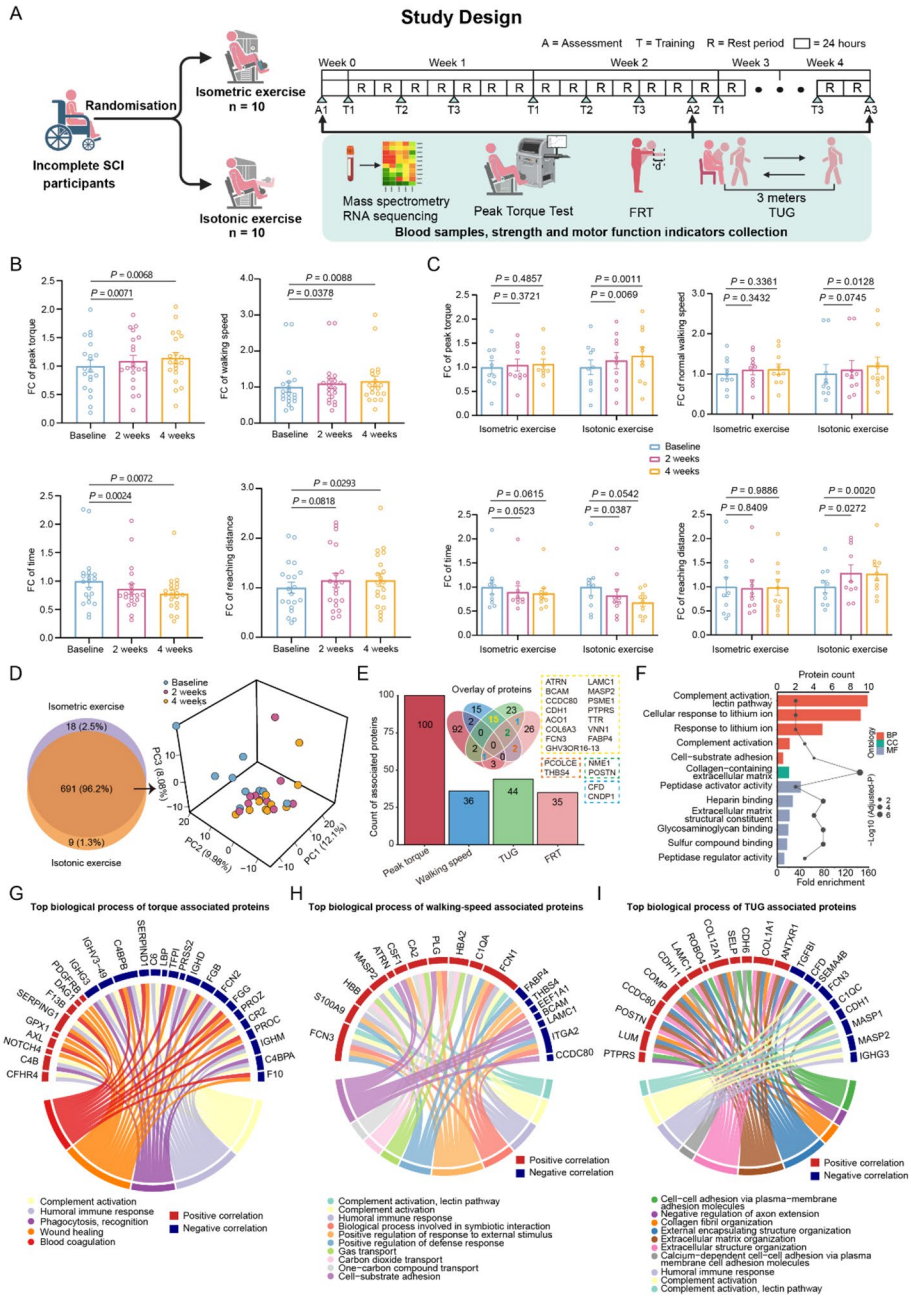

Fig. 1 (See legend on previous page.)

at 90°, participants were instructed to clench their fist and extend it forward as far as possible without taking a step. The difference in distance between the starting and ending positions of the third metacarpal bone and the wall was recorded as the value of the FRT. Participants performed three reaching attempts, and the average value of the last two trials was calculated and considered as the result of the FRT.

Timed Up and Go

Participants were seated in a chair with a backrest positioned at the beginning of a 3-m grid. If needed, they held walking aids such as canes or walk frames in their hands. Following their usual walking gait, participants walked forward for 3 m until they passed a marker. Then, they turned around and walked back to the chair, sat down, and leaned against the chair's backrest. The assessor

recorded the time starting from when the participants' back left the backrest of the chair until they sat down again. The procedure was repeated twice, and the average time from the two tests was calculated and taken as the result of the TUG.

Human blood sampling and processing

Blood sampling was performed prior to each assessment of clinical outcomes. To ensure research precision, participants were instructed to fast for 8 h prior to blood collection. Before the clinical outcome assessments, 5-ml blood samples were collected by drawing venous blood from the participant's median cubital vein and transferring it into vacutainer tubes containing EDTA (BD, 367,525). Plasma fraction was collected after centrifugation at 1300*g* at 4°C for 10 min, aliquoted, and stored at − 80°C until use. PBMC were prepared immediately by Ficoll density gradient centrifugation (Cytiva, 17144003). Aliquots of 1×10^6 dry cell pellets were frozen in liquid nitrogen until use for RNA-seq.

Animals

For this study, C57BL/6J mice (Charles River, China) were kept in randomized groups of 5 mice, before any exercise or plasma injections. All mice were housed in a temperature- and humidity-controlled environment on a 12-h light/12-h dark cycle (8 a.m. and 8 p.m.), with ad libitum access to food and water. And all groups within one experiment contained individual mouse with the same strain and sex, showing similar body weight and age. The animal study was carried out in compliance with the Animal Research: Reporting of In Vivo Experiments guidelines and the ARRIVE guidelines, as overseen by the Institutional Animal Care and Use Committee of youshulife Co. (YS-m202212001).

Ladder-climbing training

The ladder-climbing exercise, as previously described [31], was implemented for C57BL/6J male mice (aged 8–10 weeks). The exercise training involved utilizing a ladder measuring 1 m in height, with grid intervals of 1 cm. The ladder was set to attain an 80° angle with the ground. The complete formal training cycle spanned over a duration of 4 weeks, encompassing rigorous training sessions conducted consecutively for 5 days per week. Subsequently, a vital period of 2 days was allocated for rest and recovery before initiating the subsequent round of training. During each day's training routine, the mice were engaged in a task that entails ascending from the bottom to the top of the ladder, followed by a brief intermission of 20 s for rest, prior to commencing the subsequent climb. This sequence was repeated precisely ten times, ensuring an adequate number of repetitions for effective training. Three days of adaptation before training was conducted by letting mice to climb up the ladder without any resistance. After the adaptation, resistance at 20% of body weight was given to the mice by adding weight on the tail for the first week. To progressively increase exercise intensity, 50%, 75%, and 100% of body weight was applied as resistance for the next 3 weeks respectively. The control group of mice was subjected to the same environmental conditions throughout the entire experimental duration, with ad libitum access to food and water. Body weight measurements were obtained at three critical time points: before the commencement of training, prior to the initiation of the third week of training, and upon completion of the entire training period. Furthermore, following the training cycle, an assessment was conducted to determine the maximum voluntary carrying capacity of the mice [32].

Plasma and tissue sample preparation from exercised mice

Ladder-climbing and control mice were euthanized 2 days after the last training. Mice were anaesthetized with 3% isoflurane in preparation for sampling. Blood samples were collected by retro-orbital bleeding in centrifuge tubes covered with EDTA (BKMAM Biotechnology Co.Ltd, 110,403,014). Plasma fraction was collected after centrifugation at 1300*g* at 4°C for 10 min, pooled together from 7 to 8 exercised or control mice, and then frozen at − 80℃ until use. While PBMC were prepared immediately by Ficoll density gradient centrifugation (Cytiva, 17,544,602), pooled from 15 exercised or control mice. Following the extraction of PBMC, a portion of 1×10^6 cells was set aside for RNA-seq, while the remaining cells were promptly utilized for injection. Additionally, the bilateral quadriceps muscles were isolated and carefully preserved at − 80℃ for subsequent utilization.

Compression spinal cord injury and plasma injection

C57BL/6J female mice (aged 8–10 weeks) were anaesthetized by intraperitoneal injection with 15 µl of a 2.5% solution of 2,2,2-tribromoethanol (Aladdin, T161626) per gram body weight in preparation for surgery. Laminectomy of a single vertebra was performed to expose the spinal cord at the level of T10. SCI was made by the application of an aneurysm clip to exert bilateral compression on the T9 to T10 segment, resulting in approximately 50% deformation, which was maintained for 30 s. Sham-injured animals were only subjected to laminectomy. The mice were returned to the home cages after recovery on a heating pad. Twice-daily manual compression of the bladders was performed until the restoration of spontaneous urination, and a water solution containing Enrofloxacin (Sangon Biotech, A507089) at a concentration of 160 mg/L was administered orally for 5 consecutive

days after injury. SCI mice were systemically treated with plasma (100 μl/injection) or PBMC (1×10^6/injection) isolated from exercised or sedentary mice starting from 14 days post injury (DPI). Plasma and PBMC were administered via intravenous tail vein injection 8 times over 24 days or 4 times over 28 days, respectively.

Behavioral/locomotor assessment

Open field test and BMS score

BMS score for locomotion was used to evaluate hind limb locomotion recovery in the SCI mice [33]. To increase the activity of the mice, the open-field test was scheduled between 7 p.m. and 9 p.m. Briefly, mice were allowed to walk freely in an open field for 4 min. The open field was a plastic square with 15-cm sidewall height and 50-cm diameter. Evaluation was performed before injury and on 2, 14, 21, 28, 35, 42, 56, 70, and 84 DPI. The scores were judged by two independent experimenters in a blinded manner. The final score was the average of the two experimenters.

Inclined plate test

The inclined plate test was employed to evaluate hindlimb strength by assessing the weight-bearing capacity of mice on 84 DPI [34]. This test involved placing each mouse horizontally on a custom-designed smooth iron plate equipped with an angle measuring device featuring an equilibrator. The side of the mouse's head was elevated by using one side of the iron plate as an axis. The maximum angle achieved by each mouse while maintaining their position for a minimum of 5 s without any slippage was recorded. Each animal underwent three trials, with a 5-min interval between each trial to minimize fatigue effects. The resulting mean inclined plate angle from the three trials was calculated and utilized as an index value to evaluate hindlimb strength.

Footprint analysis

Footprint analysis was utilized to evaluate body weight support and physical coordination in mice on 84 DPI [35]. To be specific, blue and red ink were applied to the forelimbs and hindlimbs of the subjects, respectively. Subsequently, the mice were permitted to pass freely through a 5-cm wide channel covered with paper. By measuring the distance between the two sides of the hind paws, the stance width was determined. Additionally, stride length was defined as the distance between the point of initial contact of one hind paw to the same paw's next initial contact. The mean stride lengths of both left and right hind limbs were calculated and used as the final stride length measurement of one gait cycle. Stance width and stride length were each evaluated across three different gait cycles, and the average value was then determined as the ultimate outcome. Finally, the frequency of toe dragging was determined by the ratio of one hind limb dragging to total footsteps of the same hind limb. To ensure accuracy, this assessment was conducted over a walking distance of more than 10 gait cycles. The result was represented by the average value derived from both hind limbs.

Sampling and histology

After finishing all behavioral test, each mouse was euthanized. The mice were perfused with 20 ml of 0.9% saline, and the right atrial appendage was cut at the same time. Once the effluent liquid became clear, a 20 ml solution of 4% paraformaldehyde (Sigma-Alorich, 158,127) was used for perfusion. The spinal cord tissue near the injury site at the T9-10 level (5 mm above and below) was then removed and fixed with 4% paraformaldehyde for 24 h. Then spinal cord tissue was dehydrated in xylene and gradient alcohol solutions, embedded in paraffin, and cut into 5-μm serial sections with a slicer. The paraffin sections were subjected to staining for various purposes. HE (Sigma-Aldrich, H3136&199,540) staining was performed to evaluate the cellular structure of the tissue. LFB (Sigma-Aldrich, L0294) staining was used to assess myelination, while cresyl violet (Solarbio, G1430) staining was employed to examine neuronal survival in anterior horn by counting Nissl bodies.

Flow cytometry

Single-cell suspensions were prepared from peripheral blood. Peripheral blood was treated with red blood cell lysis buffer and resuspended in cell staining buffer. After incubation with Zombie UVTM Dye (BioLegend, 422234) for 10 min at room temperature, the cells were washed and resuspended in cell staining buffer and then stained with anti-mouse CD16/32 (BioLegend, 101319) for 10 min to block non-specific sites. Then the cells were stained with CD45-APC (BioLegend, 103116), NK1.1-PE (BioLegend, 108707), B220-BV510 (BioLegend, 103248), CD27-PerCP-Cy5-5 (BioLegend, 124213), CD38-FITC (BioLegend, 102705), CD3-BV421 (BioLegend, 100228), CD4-BV605 (BioLegend, 100547), CD8-PE-CY7 (BioLegend, 100722), CD25-BV785 (BioLegend, 102051), CD69-BV711 (BioLegend, 104537) or CD45-APC-CY7 (BioLegend, 103116), CD11b-PerCP-Cy5-5 (BioLegend, 550993), F4/80-BV711 (BioLegend, 123147), CD80-APC (BioLegend, 104714), Ly6G-BV510 (BioLegend, 127633) at 4℃ for 30 min. After washing with cell staining buffer, the cells needed to be performed intracellular staining were fixed and permeabilized in fixation buffer and then stained with CD206-PE (BioLegend, 141706) for 20 min at room temperature.

Samples were analyzed on the BD LSR Fortessa™ X-20 cell analyzer (BD, USA), with 10,000 targeted events acquired.

Plasma proteomic sample preparation and processing

The frozen human/mouse plasma samples were allowed to thaw at room temperature for 30 min, and subsequent high-abundance protein depletion was performed using Pierce Top 14 Abundant Protein Depletion Spin Columns (Thermo Fisher Scientific, A36369). Ten microliters of the plasma sample was diluted with 50 mM NH4HCO3 and subjected to centrifugation at 14,000*g* for 20 min at 20°C using Millipore 10 kDa cutoff filter units. This process was repeated three times. Following that, the sample was reduced by adding a final concentration of 10 mM dithiothreitol (DTT; Sigma-Aldrich, D0632-1G) and incubated at room temperature for 1 h. Subsequently, the sample was alkylated in the dark by adding a final concentration of 55 mM iodoacetamide (IAA; Sigma-Aldrich, A3221) and incubating at room temperature for 1 h. To exchange the solvent of the protein mixtures, centrifugation at 14,000*g* for 20 min at 20°C was performed three times using 50 mM NH4HCO3. The proteins were then digested overnight at 37°C using sequencing grade modified trypsin (Promega, V5113) at a protein-to-enzyme ratio of 50:1. Tryptic peptides were collected by centrifugation at 14,000*g* for 20 min at 20°C. The tryptic peptides were treated with 1% trifluoroacetic acid (TFA; Sigma-Aldrich, T6508) and purified using C18 Ziptips. Elution was performed with 0.1% TFA in 50–70% acetonitrile. The eluted peptides were lyophilized using a SpeedVac (Thermo Fisher Scientific, USA) and re-suspended in a solution of 1% formic acid and 5% acetonitrile. Prior to analysis, iRT peptides (Biognosys, Switzerland) were spiked into the sample following the manufacturer's instructions to serve as internal retention time standards.

The peptides were re-dissolved in solvent A (A: 0.1% formic acid in water) and analyzed by Orbitrap Exploris 480 with a FAIMS coupled to an EASY-nano-LC 1200 system (Thermo Fisher Scientific, USA). For the analysis, 2 µL of the peptide sample was loaded onto a 25-cm analytical column with a 75-µm inner diameter, packed with 1.9 µm resin (Dr Maisch, Germany). The peptides were separated using a 120-min gradient starting at 6% buffer B (80% acetonitrile with 0.1% formic acid). The gradient profile consisted of stepwise increases to 20% over 99 min, followed by a step to 32% for 5 min, a step to 80% for 1 min, and a subsequent 5-min hold at 80%. Throughout the analysis, the column flow rate was maintained at 600 nl/min, and the column temperature was set to 55°C. The electrospray voltage was set to 2 kV to facilitate ionization and subsequent analysis.

Proteomics data acquisition and processing

The mass spectrometer was operated in DIA mode using a hybrid data strategy [36]. Briefly, a survey scan was performed with a resolution of 120,000, a normalized automatic gain control (AGC) target of 3e6, and a maximum injection time of 20 ms. For the DIA MS2 acquisition, variable isolation windows were implemented with specific window widths: 30 m/z for a mass range of m/z 350–408 (2 windows), 10 m/z for a mass range of m/z 408–795 (43 windows), 20 m/z for a mass range of m/z 795–985 (11 windows), and 50 m/z for a mass range of m/z 985–1200 (4 windows). Each full scan was followed by 20 windows with a resolution of 30,000, a normalized AGC target of 1e6, and stepped normalized collision energy values of 25.5, 27, and 30. Compensation voltages (CV) of − 45 and − 65 V were selected and applied to the MS/MS scans and the corresponding survey scan.

The raw data obtained from DIA were processed and analyzed using Spectronaut 14 software (Biognosys, Switzerland) with the default settings for dDIA analysis. The retention time prediction type was set to dynamic iRT, which utilizes an adaptive approach to predict retention times. Spectronaut was configured to search the target database UP000005640, assuming trypsin as the digestion enzyme. Carbamidomethylation (C) was specified as the fixed modification, while oxidation (M) was defined as a variable modification. Data extraction parameters were determined by Spectronaut based on extensive mass calibration. The software dynamically determines the optimal extraction window size based on iRT calibration and gradient stability. To control for false discoveries, a cutoff of 1% was applied for both precursor and protein-level false discovery rate (FDR). Decoy generation was set to "mutated," which is like scrambling but involves randomly swapping positions of amino acids within a peptide (with a minimum of 2 swaps and a maximum of half the length of the peptide). Normalization strategy was set to global normalization, ensuring harmonization across samples. The major group quantities were calculated based on the average of the top three filtered peptides that passed the FDR cutoff.

Plasma metabolomics sample preparation and processing

The plasma sample was stored at − 80°C in a refrigerator until thawed on ice and vortexed for 10 s. Subsequently, 50 µl of the sample and 300 µl of extraction solution (ACN: Methanol = 1:4, V/V), containing internal standards, were added to a 2-mL microcentrifuge tube. The mixture was then vortexed for 3 min and centrifuged at 12,000 rpm for 10 min at 4°C. Following centrifugation, 200 µl of the resulting supernatant was collected and placed at − 20°C for 30 min before undergoing another

round of centrifugation at 12,000 rpm for 3 min at 4°C. From this, 180-µl aliquots of the supernatant were extracted for LC–MS analysis.

The sample extracts were analyzed using an LC–ESI–MS/MS system (SCIEX, USA). The analytical conditions were as follows, UPLC: column, Waters ACQUITY UPLC HSS T3 C18 (1.8 µm, 2.1 mm*100 mm); column temperature, 40°C; flow rate, 0.4 mL/min; injection volume, 2 µL; solvent system, water (0.1% formic acid): acetonitrile (0.1% formic acid); gradient program, 95:5 V/V at 0 min, 10:90 V/V at 11.0 min, 10:90 V/V at 12.0 min, 95:5 V/V at 12.1 min, 95:5 V/V at 14.0 min. A triple quadrupole-linear ion trap mass spectrometer (QTRAP; SCIEX, USA) was used for LIT and triple quadrupole (QQQ) scans. The QTRAP® LC–MS/MS System, equipped with an ESI Turbo Ion-Spray interface, operated in both positive and negative ion mode and controlled by Analyst 1.6.3 software. The ESI source operation parameters were as follows: source temperature 500°C; ion spray voltage (IS) 5500 V (positive), −4500 V (negative); ion source gas I (GSI), gas II (GSII), curtain gas (CUR) was set at 55, 60, and 25.0 psi, respectively; the collision gas (CAD) was high. Instrument tuning and mass calibration were performed with 10 and 100 µmol/L polypropylene glycol solutions in QQQ and LIT modes, respectively. Specific multiple reaction monitoring (MRM) transitions were monitored for each period based on the elution profile of the metabolites.

Metabolomics MS-data processing and compound identification

Based on the self-built database MetWare Database (http://www.metware.cn/), the materials were qualitatively analyzed according to the secondary spectrum information. Briefly, based on the self-built metabolite database, mass spectrometry was employed for both qualitative and quantitative analysis of the metabolites present in the samples. MRM mode in the chromatogram was utilized to visualize a multi-peak graph, where each differently colored peak represented a detected metabolite. To identify the substances, specific characteristic ions for each metabolite were selected using triple quadrupole screening. The signal intensities, measured in counts per second (CPS), were captured by the detector. These mass spectrometry files of the samples were then processed using the MultiQuant software, which facilitated peak integration and calibration. The software performed peak integration and calculated the peak area for each chromatographic peak, reflecting the relative content of the corresponding substance. This allowed for an estimation of the abundance or concentration of the detected metabolites. Finally, all the integrated peak area data were exported and saved for further analysis and interpretation.

RNA-sequencing processing and analyses

Total RNA was extracted using the Trizol Reagent (Invitrogen Life Technologies, 15596026), followed by assessment of its concentration, quality, and integrity using a NanoDrop spectrophotometer (Thermo Fisher Scientific, USA). For RNA sample preparations, 3 µg of RNA was utilized as input material. The generation of sequencing libraries was carried out with the TruSeq RNA Sample Preparation Kit (Illumina, RS-122–2001). In brief, poly-T oligo-attached magnetic beads were employed to purify mRNA from the total RNA. Fragmentation of the mRNA was achieved under elevated temperature using divalent cations in an Illumina proprietary fragmentation buffer. First-strand cDNA synthesis was performed using random oligonucleotides and SuperScript II. Subsequently, second-strand cDNA synthesis was conducted using DNA Polymerase I and RNase H. The resulting overhangs were converted into blunt ends through exonuclease/polymerase activities, and the enzymes were subsequently removed. Following adenylation of the 3′ ends of the DNA fragments, Illumina PE adapter oligonucleotides were ligated to facilitate hybridization. To select cDNA fragments of approximately 400–500 bp in length, the library fragments were purified using the AMPure XP system (Beckman Coulter, USA). DNA fragments with ligated adaptor molecules on both ends were then selectively enriched via a 15-cycle PCR reaction using the Illumina PCR Primer Cocktail. The resulting products were purified once again using the AMPure XP system and quantified using the Agilent high sensitivity DNA assay on a Bioanalyzer 2100 system (Agilent, USA). Finally, the sequencing library was sequenced on NovaSeq 6000 platform (Illumina, USA) by Shanghai Personal Biotechnology Cp. Ltd.

Multi-omics preprocessing and normalization

For proteomic data, each pairwise group independently conducted a filtration process on 14 types of high-abundance proteins and proteins exhibiting more than a 50% rate of missing values. The metabolomic data underwent filtering based on removal criteria involving CV values of quality control samples exceeding 30% and missing values of overall samples surpassing 50%. For transcriptomic data, an effective expressed gene required count greater than 0 in more than 50% of all samples. The missing values of the retained proteins or metabolites were imputed through the application of the random forest method in the "missforest" R package. The proteome or metabolome was then subjected to normalization via the vsn method, using the "vsn" R package. While counts per

million mapped reads (CPM) were utilized to measure the relative abundance of the transcripts in the "edgeR" R package.

Dimension reduction and clustering

The vsn-normalized data or log2-transformed CPM served as the basis for unsupervised multivariate statistical analysis, employing PCA ("promor" R package) and tSNE ("Rtsne" R package). Meanwhile, supervised multivariate statistical analysis was executed utilizing sPLS-DA via the "mixOmics" R package. OPLS-DA of metabolomic profiling was generated using the "ropls" R package with the following parameters: permutation = 10,000, cross-validation = 15, scale = center. The normalized data of DEPs and DEMs were used for the unsupervised hierarchical clustering analysis in the "pheatmap" R package.

Identification of exercise-responsive substance

For the analyses of the human plasma proteome or PBMC transcriptome, a robust linear regression model adjusted for the individual characteristics, incorporating gender, age, weight, injury classification, and months post injury, in the "limma" R package was used to find exercise-responsive proteins or genes. Adjustment of *P*-values was performed using the Benjamini-Hochberg (BH) procedure. Proteins displaying $|\log2(FC)| > \log2(1.2)$ and an adjusted *P*-value < 0.05 were identified as DEPs. Genes displaying $|\log2(FC)| > \log2(2)$ and an adjusted *P*-value < 0.05 were identified as DEGs. For the analyses of mouse proteome, metabolome, and transcriptome, differentially expressed mRNAs, proteins, and metabolites were also detected using the "limma" R package. *P*-values were corrected for multiple hypotheses using the BH method.

Dynamic expression analysis

For the plasma proteomic data, a fuzzy c-means algorithm of the "Mfuzz" R package was applied to cluster the proteins according to their dynamic expression patterns. A robust linear regression model adjusted for the individual characteristics, incorporating type of training, gender, age, weight, injury classification, and months post injury, in the "limma" R package was used to find candidate proteins. Proteins displaying an adjusted *P*-value < 0.05 were identified as candidate proteins and included in the clustering analysis.

Immunocyte infiltration analysis

To investigate the changes in peripheral blood immune cell composition in incomplete SCI patients following the training, we utilized a deconvolution method to quantify the proportions of 22 human blood cell types from bulk RNA-seq samples with the "CIBERSORT" R package [37]. We then compared the alterations in blood cell proportions before and after exercise in each training groups, respectively.

Correlation and network analysis

The "ppcor" R package facilitated Spearman's partial correlation examination, with control variables constituting sex, age, weight, and months post injury. Spearman's rank correlations were calculated using the "psych" R package, and weighted, undirected networks were plotted with "igraph" R package, while Mantel's test between protein sets and DEMs was performed by "vegan" R package. A threshold for statistical significance was set at a *P*-value < 0.05.

Pathway enrichment analysis

Over-representation analyses were implemented through the KEGG and GO databases, accomplished using the "clusterProfiler" R package. Pathway significance was assessed applying a hypergeometric test, with the BH method employed for multiple testing correction, setting statistical significance adjusted *P*-values < 0.05. Ingenuity pathway analysis (IPA) platform (QIAGEN, Germany) was also used to search for enriched pathways. Significance of pathways was determined by the hypergeometric test (one-sided) in IPA, setting statistical significance *P*-values < 0.05. GSEA was also performed with the "clusterProfiler" R package. Molecular Signatures Database (MSigDB) of hallmark gene sets, curated gene sets, and ontology gene sets were used for enrichment analysis. The number of permutations was set to 10,000 and statistical significance was set at *P*-values < 0.05.

Statistical analysis

All values in figures were shown as mean ± SEM, mean ± SD or median (IQR). Statistical analysis was performed with GraphPad Prism (Version 9.5.1), SPSS (Version 23.0), or R (Version 4.2.3) unless stated otherwise. Area of demyelination and number of Nissl bodies were analyzed by using Fiji software (ImageJ). The flow cytometry data were analyzed and plotted using Flow Jo (Version 10.8.1). For comparisons between two groups, continuous data were analyzed using an unpaired, two-sided Student's *t* test. Categorical data, on the other hand, were tested using either the chi-squared test or Fisher's exact test, as appropriate. In human clinical trials involving repeated measurements, one-way repeated measures analysis of variance (ANOVA) with Dunnett's multiple comparisons test was conducted to identify significant differences among three groups. In animal experiments, one-way ANOVA or two-way ANOVA with Tukey's multiple comparisons test was performed to identify significant differences among three or more groups. A

significance level of P-value < 0.05 was considered significant (*P < 0.05, **P < 0.01, ***P < 0.001, and ****P < 0.0001).

Results

Muscle strength, ambulation, and balance ability improve with resistance exercise in incomplete SCI patients

To investigate the rehabilitative effects of resistance exercise on locomotor function in SCI patients, we conducted a 4-week clinical trial (Fig. 1A). A total of 20 patients with incomplete SCI were enrolled and completed the procedures (Additional file 2: Fig. S1). The cohort's average age was 43.1 ± 10.0 years, with a median post-injury duration of 5.5 (3.75–11) months. The participants were randomly assigned to two experimental groups: isometric resistance exercise and isotonic resistance exercise. Following randomization, there were no significant differences in baseline characteristics between the two groups (Additional file 2: Table. S1). As expected, it was demonstrated the patient's muscle strength (peak torque of quadriceps femoris) progressively increased with the duration of training (Fig. 1B). To comprehensively assess lower limb locomotor function, we employed three clinical tests: FRT for static balance ability, TUG test for dynamic balance ability, and 10 MWT for ambulation ability, which were demonstrated the reliability and consistency when mutually corroborated each other (Additional file 1: Fig. S1A-C). Of note, all clinical outcomes related to locomotor function showed significant improvement after just 2 weeks of intervention, and these improvements were maintained until the end of the trial (Fig. 1B). Furthermore, we made another intriguing discovery that the change in peak torque of the target muscle showed only weak correlations with walking speed (Spearman's rho = 0.3132, P = 0.0491) and no significant correlations with the other clinical outcomes (FRT and TUG) (Additional file 1: Fig. S1D-F). Together, these findings imply that the resistance exercise-induced improvements in ambulation and balance function are not primarily driven by the enhancement of target muscle strength. While a subgroup analysis of the two resistance exercise patterns revealed that both cohorts of patients demonstrated progressive improvements in muscle strength, walking performance, and balance abilities throughout the course of the intervention (Fig. 1C). Furthermore, isotonic exercise resulted in a remarkable increase in target muscle strength, whereas isometric exercise demonstrated limited improvements (Additional file 1: Fig. S1G). Similarly, isotonic exercise training had shown superiority over isometric resistance training in the recovery of ambulation and balance abilities as well (Additional file 1: Fig. S1H-J), suggesting that isotonic exercise training is a superior approach compared to isometric exercise training in promoting locomotor function recovery in incomplete SCI patients.

Plasma proteome associated with changes in locomotor function focuses on humoral immune response and complement activation

To systematically analyze underlying blood substance associated with changes with locomotor function, data-independent acquisition mass spectrometry (DIA-MS)-based proteomics for plasma was performed, and 788 proteins were identified in total. To ensure the technical reproducibility of the study, rigorous quality control was implemented. The number of proteins detected in each sample did not exhibit a significant difference across the different time points. However, it is worth noting that one sample showed a notably lower protein detection, with only 532 proteins identified, whereas the average for the remaining samples was 694 ± 19 proteins (Additional file 1: Fig. S2A). Following Pearson's and Spearman's correlation analyses, it was observed that the correlation exhibited by this specific sample deviated significantly from the rest of the samples (Additional file 1: Fig. S2B, C). Thus, we identified this sample as an outlier and excluded it from subsequent analyses. Consequently, 29 samples were included in the final analysis, and a total of 709 plasma proteins were integrated into in the isometric exercise group, and 700 plasma proteins were included in the isotonic exercise group, with 691 proteins in common (Fig. 1D). Though t-distributed stochastic neighbor embedding (tSNE) scatterplots displayed noticeable heterogeneity among the patients (Additional file 1: Fig. S2C), principal component analysis (PCA) and sparse partial least squares discriminant analysis (sPLS-DA) revealed a slight but clear variance between samples of baseline and post-exercise (Fig. 1E and Additional file 1: Fig. S2D). Meanwhile, the coefficient of variation (CV) showed no significant difference between the two treatment groups, indicating stability of the two interventions (Additional file 1: Fig. S2E). PCA analyses did not exhibit significant variance of proteomics between post-exercise and sedentary conditions respectively, subsequent sPLS-DA showed significant variance in each group (Additional file 1: Fig. S2F, G). These quality control analyses confirmed the integrity and validity of the dataset prior to the in-depth proteomic profiling.

Given the substantial patient heterogeneity, partial correlation analysis was employed to identify plasma proteins associated with various clinical outcomes, with controlled variables including gender, age, weight, and the months of post-injury. As a result, we identified 100 proteins partial-correlated with change of peak torque, as well as 36, 44, and 35 proteins with normal walking speed, TUG performance, and FRT performance,

respectively (Fig. 1E). Despite the absence of completely overlapping regions among the four kinds of associated proteins, we still identified 21 proteins that overlap among the three locomotor function-related proteins, with two of these proteins being associated with all three locomotor functions (Fig. 1E). Subsequent Gene Ontology (GO) enrichment analysis also revealed that these overlapping proteins primarily activated the complement pathway (Fig. 1F). The results of the GO analysis revealed that although the proteins associated with FRT did not exhibit significant pathway enrichment, the other three kinds of proteins associated with clinical outcomes demonstrated enrichment in shared pathways, such as the humoral immune response and complement activation pathways (Fig. 1G–I). Additionally, the proteins associated with peak torque were enriched with biological processes related to coagulation pathway and wound healing (Fig. 1G). Notably, the proteins involved in the pathways of humoral immune response and complement activation exhibited predominantly positive correlations with walking velocity and negative correlations with TUG performance, respectively (Fig. 1H, I). Collectively, our findings provide support for the crucial roles of the proteins involved in complement activation and humoral immune response in mediating the recovery of locomotor function in individuals with incomplete SCI.

Plasma proteome highlight signatures of resistance exercise-induced immunomodulation in incomplete SCI

As a limited variance between the samples collected at 2 weeks and 4 weeks identified by PCA, the samples from both time points were combined to set a post-exercise group to identify proteins that exhibit stable and sustained changes following exercise. Due to the heterogeneity of patients, proteins significantly affected by resistance exercise were identified using a robust linear regression model adjusted for baseline characteristics, including age, gender, weight, types of resistance exercise, months of post-injury, and classification of injury. As a result, it was identified 56 significantly upregulated exercise-responsive proteins and 40 downregulated exercise-responsive proteins [fold change (FC) > 1.2, adjusted *P*-value < 0.05] following resistance exercise intervention compared with baseline. The hierarchical clustering analysis of the resistance exercise-responsive differentially expressed proteins (DEPs) showed distinguishable expression patterns over time (Fig. 2A). Although only a few DEPs (19/96) were previously identified to be associated with locomotor function, GO enrichment still yielded noteworthy findings (Additional file 1: Fig. S2H). Notably, the GO analysis revealed that the upregulated DEPs were significantly enriched in key biological processes associated with complement activation, coagulation, and humoral immune response (Fig. 2B). Likewise, the downregulated proteins also showed enrichment in biological processes related to complement activation and coagulation (Fig. 2B). Consistently, Kyoto Encyclopedia of Genes and Genomes (KEGG) pathway analysis was performed to identified complement and coagulation cascades as the underlying signaling pathways in response to resistance exercise (Additional file 1: Fig. S2I). Thus, we marked 11 DEPs involved in complement pathways and humoral immune response, including CD59, MBL2, SERPING1, CAMP, C1QB, C1QA, C4BPA, MASP1, LTF, CFHR1, and C8A (Fig. 2C). Of note, CD59 and C4BPA are inhibitors of complement pathway, and their downregulation suggests an intensified activation of the complement pathway. Moreover, gene set enrichment analysis (GSEA) of proteomics data further confirmed that lectin pathway induced complement activation was activated (NES = 1.73, *P*-value = 0.007) (Fig. 2D). Additionally, we also uncovered that signaling pathways contributing to tissue regeneration were activated, including positive regulation of endothelial cell proliferation, sprouting angiogenesis, and regulation of vasculature development, which was a common adaption to exercise [7, 38, 39] (Fig. 2D). Our study revealed a significant discovery that short-term resistance exercise in individuals with incomplete SCI elicited an inhibitory effect on platelet activity, akin to the effects observed with regular exercise in previous studies [40–42] (Fig. 2D). To further investigate the changes in the dynamic expression patterns induced by resistance exercise, we employed fuzzy c-means method to cluster the time-dependent proteins. A total of 114 time-dependent candidate proteins were categorized into four clusters (Fig. 2E). Cluster 2, which was persistently upregulated, exhibited enrichment in pathways related to acute inflammatory responses, complement activation, and axonogenesis regulation (Fig. 2F). Interestingly, Cluster 4, characterized by a predominance of downregulated proteins, was enriched in pathways related to humoral immune responses and complement activation (Fig. 2F). Notably, the proteins enriched within these pathways were primarily composed of inhibitory factors. An overlap of 79 proteins was identified between time-dependent proteins and resistance exercise-responsive proteins (Additional file 1: Fig. S2J). Notably, both upregulated and downregulated overlapping proteins were enriched in pathways associated with complement activation and humoral immunity (Additional file 1: Fig. S2K, L). This finding further supports the notion that resistance exercise exerts a sustained and

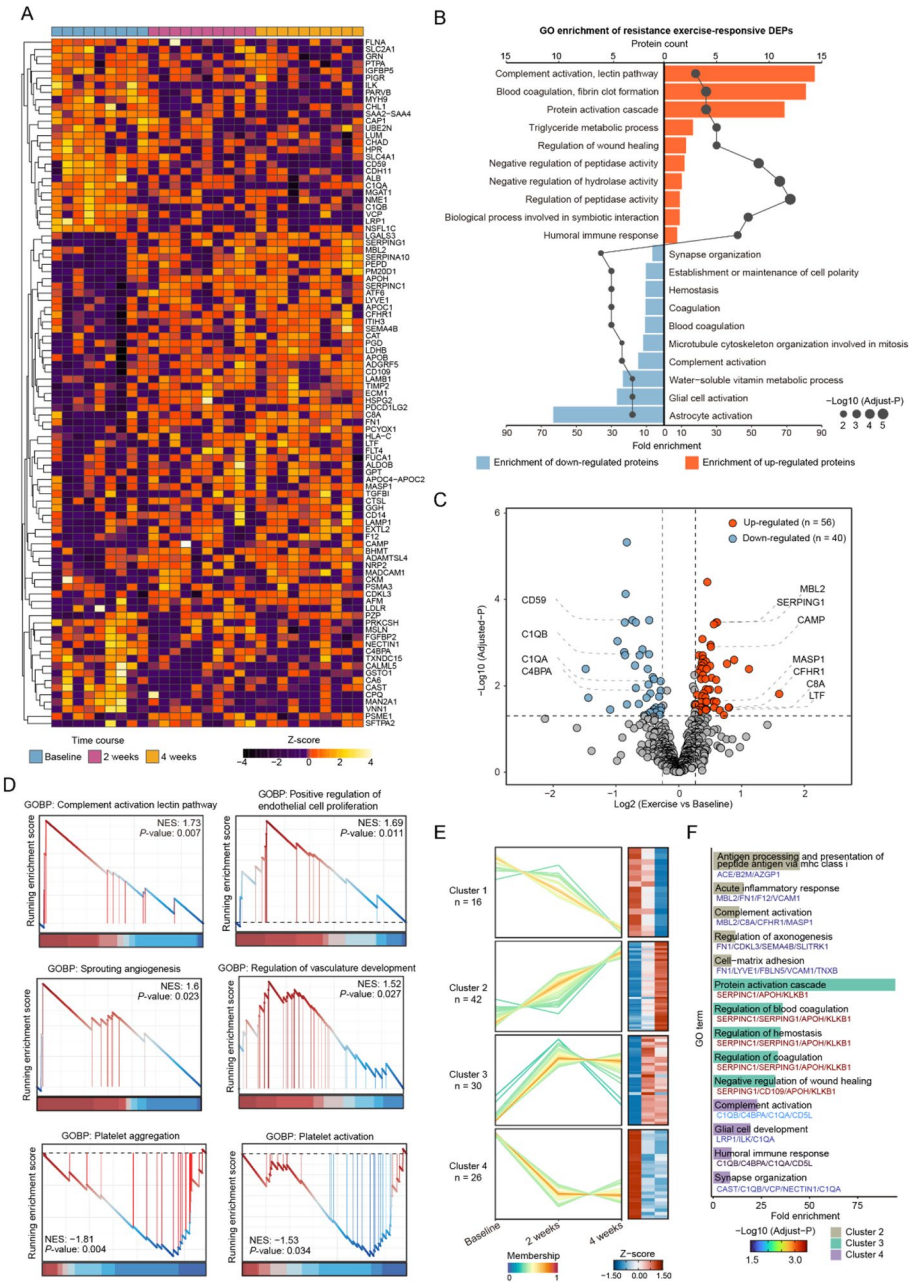

Fig. 2 Exploration of exercise-responsive proteins and functional enrichment analysis in human. **A** Heatmap showing hierarchical clustering analysis of resistance exercise-responsive differentially expressed proteins (DEPs) over time. **B** Bar plot showing top enriched terms based on GO enrichment analysis of the upregulated and downregulated DEPs. The bar represents the fold enrichment factor, and the line graph indicates the count of proteins enriched by the pathway. **C** Volcano plot showing the resistance exercise-responsive differently expressed proteins (DEPs) across all the post-exercise samples. **D** Gene set enrichment analysis (GSEA) of resistance exercise-responsive signaling pathways and BP based on ontology gene sets. **E** Line plots of standardized abundances of plasma candidate proteins following mFuzz clustering. Candidate proteins were identified across three time-points if they presented a Benjamini–Hochberg (B–H) adjusted *P*-value of less than 0.05, as determined by a robust linear regression model. **F** Bar plot showing top enriched terms based on GO enrichment analysis of time-dependent proteins in each cluster. The bar represents the fold enrichment factor. The enriched proteins are listed under each respective pathway, with the font color of the protein names indicating the significance of the adjusted *P*-values

time-dependent immunomodulatory effect in patients with incomplete spinal cord injury.

Plasma proteome and PBMC transcriptome reveal distinct forms of immunomodulation associated with different types of resistance exercise

Given the notable divergence in the restorative effects of isometric resistance and isotonic resistance on locomotor function, our aim was to ascertain potential similarities or dissimilarities in the physiological responses elicited by the two exercise modalities. The observed positive correlation (rho = 0.224, *P*-value < 0.0001) in the changes of proteins between the two groups suggested a degree of similarity in the plasma protein responses to both distinct modes of resistance exercise (Fig. 3A). Then, we identified 57 DEPs in the isometric exercise group and 52

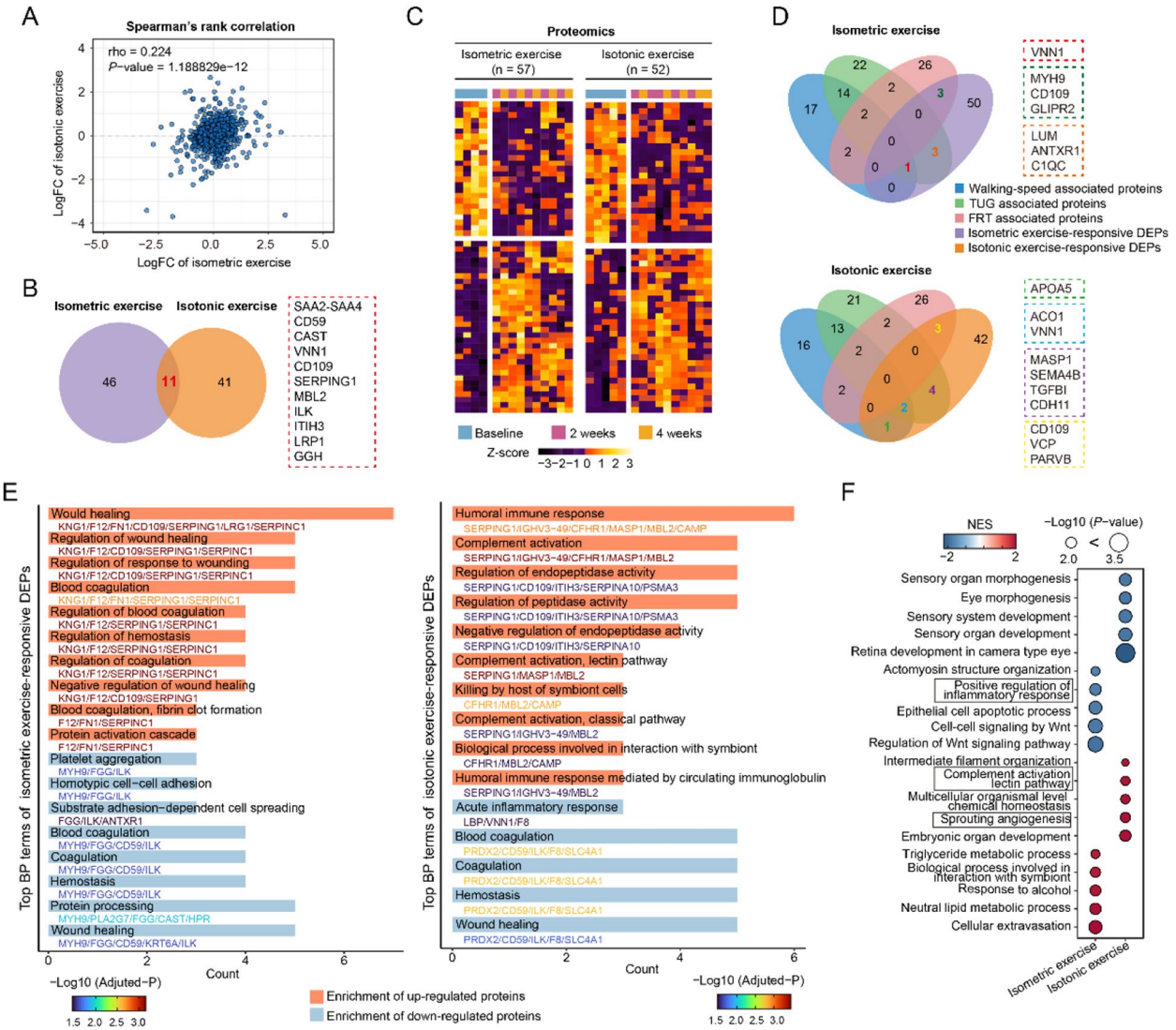

Fig. 3 Differential proteomic changes induced by various resistance exercises. **A** Scatter plots showing Spearman's rank correlation of proteomic changes between isometric exercise and isotonic exercise groups. **B** Venn diagrams showing the overlap between isometric and isotonic exercise-responsive DEPs. The proteins listed within the red box are those that overlap between the two groups. **C** Heatmap showing scaled abundance of isometric or isotonic exercise-responsive DEPs. **D** Venn diagrams showing the overlap within three kinds of clinical outcome-associated proteins and isometric or isotonic exercise-responsive DEPs. The proteins listed within the box represent the overlapping regions of the Venn diagram, with the color of the box corresponding to the colors of the numbers displayed within the diagram. **E** Top enriched BP terms based on GO enrichment analysis of isometric exercise-responsive and isotonic exercise-responsive DEPs. The bars represent the count of enriched proteins, with the enriched proteins listed beneath each corresponding pathway. The font color of the protein names indicates the significance of the adjusted *P*-values. **F** Bubble plot presenting the enriched pathways identified through GSEA in subgroups based on ontology gene sets, including both activated (Red) and suppressed (Blue) pathways

DEPs in the isotonic exercise group, with only 11 proteins shared between the two groups (Fig. 3B). The hierarchical clustering analysis revealed exercise-induced DEPs in the two groups exhibited significant and sustained changes after exercise, respectively (Fig. 3C). Despite the lower number of differentially expressed proteins (DEPs) induced by isotonic exercise compared to isometric exercise, it is worth noting that 10 DEPs showed correlations with changes in locomotor functional outcomes in the isotonic exercise group, while only 7 DEPs were identified in the isometric exercise group (Fig. 3D). These findings supported the finding above that isotonic exercise had a more significant impact on the alterations of locomotor function following incomplete SCI. Furthermore, isotonic exercise-responsive DEPs tended to be enriched in pathways related to activation of complement and humoral immune responses, whereas isometric exercise-responsive DEPs were more likely to be enriched in coagulation pathways (Fig. 3E). GSEA provided further confirmation of the distinct pathway enrichment induced by the two different modes of resistance exercise. Isotonic exercise activated several top pathways known to be beneficial for tissue healing, including lectin pathway induced complement activation and sprouting angiogenesis; however, isometric exercise indicated a suppression of the positive regulation of the acute inflammatory response (Fig. 3F).

Based on our significant findings regarding the impact of resistance exercise on systemic immune response of incomplete SCI, we further aimed to investigate whether peripheral blood mononuclear cells (PBMC) transcriptome exhibit distinct post-exercised trends using RNA-sequencing (RNA-seq). After quality control was implemented, our analysis of RNA-seq revealed 337 differentially expressed genes (DEGs) in the isometric exercise group and 216 DEGs in the isotonic group (Additional file 1: Fig. S3A-F). Although the GO enrichment analysis for DEGs did not identify statistically significant pathways, GSEA was still able to reveal similar regulation of immune function in PBMC following exercise in the two groups, including suppression of B cell homeostasis, activation of T-cell function, and activation of inflammation response (Additional file 1: Fig. S3G). Notably, isotonic exercise demonstrated a propensity to activate monocyte/macrophage function, whereas isometric exercise displayed a predilection towards stimulating neutrophil function. Hence, isotonic exercise appeared to be more favorable for activating innate immunity. As complement proteins are important effector proteins within the innate immune system, the PBMC RNA-seq analysis aligned with the findings from the plasma proteome. In addition, we further employed deconvolution methods to explore the compositional changes of peripheral immune cells (Additional file 1: Fig. S3H). In patients undergoing isometric resistance exercise, no significant changes were observed in the proportion of immune cells (Additional file 1: Fig. S3I). In contrast, those participating in isotonic exercise showed a significant increase in the proportion of $CD8^+$ T cells (Additional file 1: Fig. S3J). In summary, the comprehensive analysis of plasma proteome and PBMC transcriptome uncovered compelling evidence of systemic immune modulation in response to two kinds of resistance exercise in incomplete SCI patients.

Resistance exercise induces systemic and local immunomodulation in mice

To mimic the physiological effects of resistance exercise, a set of wild-type mice was subjected to a 4-week weight-loaded ladder-climbing training (Fig. 4A, B). After 4 weeks of training, the exercised mice demonstrated significant reductions in body weight gain and substantial increases in maximum load capacity compared to the sedentary group (Fig. 4C, D). Subsequently, proteomic profiling using DIA-MS was performed, resulting in the identification of a total of 1032 proteins. PCA and sPLS-DA of the plasma proteome revealed clear variance between the two conditions, indicating robust plasma proteome changes in response to exercise (Additional file 1: Fig. S4A, B). The CV within the two conditions for the proteome was relatively similar, suggesting comparable overall variability (Additional file 1: Fig. S4C). As a result, 36 upregulated DEPs and 57 downregulated DEPs were identified ($FC > 1.5$, adjusted P-value < 0.05), hierarchical clustering analysis of which revealed distinct patterns of changes induced by the exercise intervention (Fig. 4E). In accordance with previous findings from the human plasma proteome, GO analysis demonstrated the enrichment of upregulated DEPs in immune-related pathways (Fig. 4F). These pathways encompassed the classical pathway-induced complement activation, B cell receptor signaling pathway, humoral immune response mediated by circulating immunoglobulin, positive regulation of B cell activation, and humoral immune response.

Notably, among the upregulated proteins, five immunoglobulin heavy chains, including IGHG2B, IGHG2C, IGHV5-12, IGHV1-31, and IGHV1-82, were key proteins enriched in relevant pathways (Fig. 4G, H). Moreover, a weighted network analysis employing Spearman's rank correlation was performed to examine the relationships among the upregulated DEPs (Fig. 4I). The immunoglobulin heavy chains exhibited the top centrality degree within the network, suggesting their potential involvement in coordinated changes with other upregulated DEPs and implying underlying functional relationships or regulatory interactions. Furthermore, PBMC and quadriceps muscle RNA-seq was performed to detect

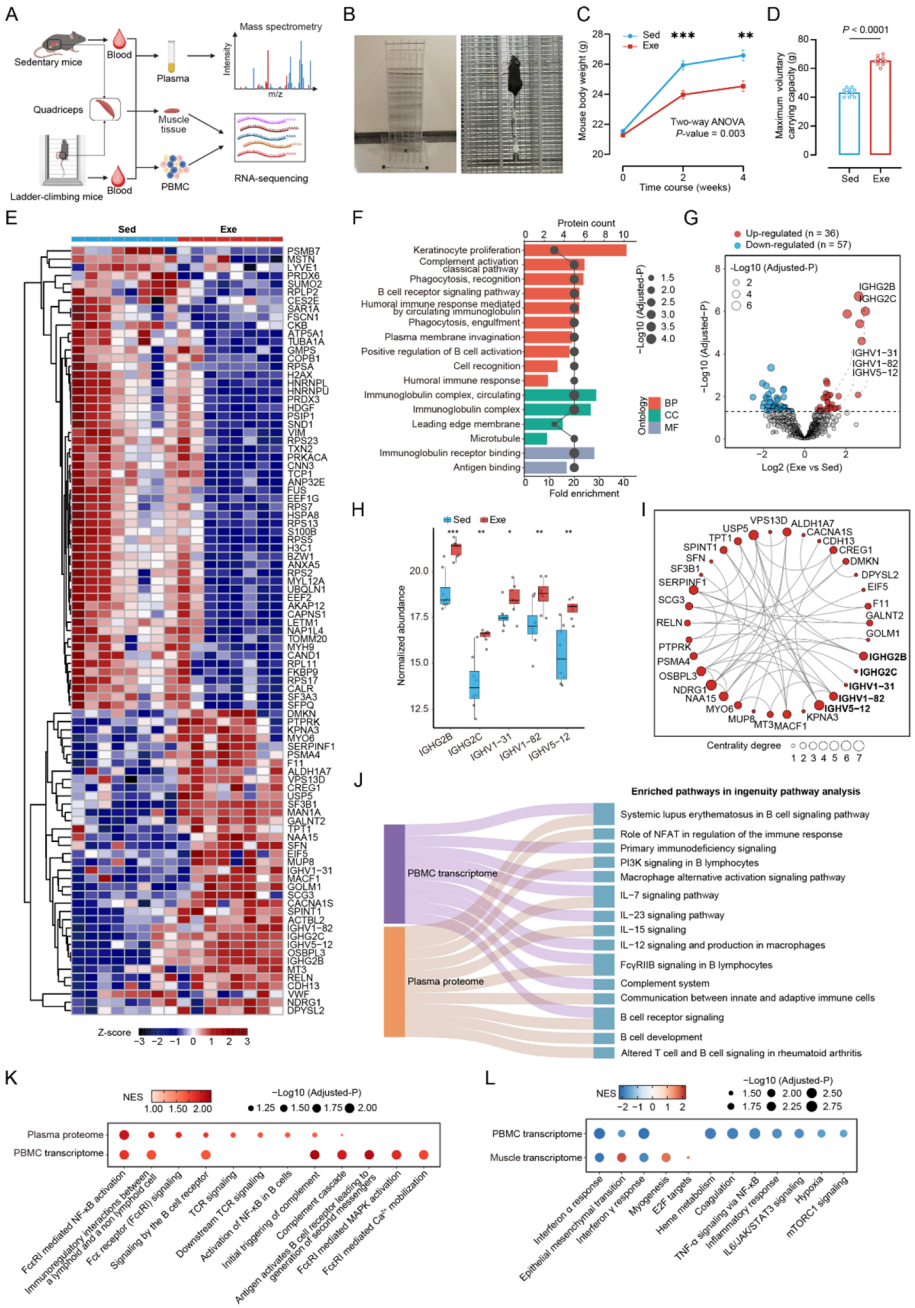

Fig. 4 Weight-loaded ladder-climbing modeling and immunomodulation in response to exercise. **A** Pattern diagram of the weight-loaded ladder-climbing mouse model (Created with BioRender). **B** Self-made 5-track training climber. **C** Line graph illustrating the changes in body weight of mice in the exercise and sedentary group. Two-way repeated measures ANOVA with Bonferroni's multiple comparisons test, $n = 15$, $^{*}P < 0.05$, $^{**}P < 0.01$, $^{***}P < 0.001$. **D** Bar plot showing mean value of maximum voluntary carrying capacity in the exercise and sedentary group. Each dot represents a sample. Data are expressed as means ± SEM, $n = 10$. *P*-values are determined by unpaired Student's *t* test. **E** Heatmap showing scaled abundance of DEPs in response to ladder climbing in mice. **F** Bar plot showing key enriched terms based on GO enrichment analysis of upregulated DEPs in plasma proteome. The bar represents the fold enrichment factor, and the line graph indicates the count of proteins enriched by the pathway. **G** Volcano plot showing the exercise-responsive DEPs in mice. **H** Box plot displaying the normalized abundance expressions of five immunoglobulin heavy chains post exercise. *P*-values were determined by unpaired Student's *t* test, $^{*}P < 0.05$, $^{**}P < 0.01$, $^{***}P < 0.001$. **I** Spearman's rank correlation networks of upregulated DEPs. Size of nodes represents their connections (Centrality degree) with the other DEPs. **J** Sankey plot presenting intersection between exercise-responsive immune pathways in peripheral blood mononuclear cells (PBMC) transcriptome (Purple) and plasma proteome (Orange) through Ingenuity pathway analysis (IPA) based on upregulated DEPs in plasma proteome and the overall DEGs in PBMC transcriptome. **K** Bubble plot displaying the activated immune pathways identified in the plasma proteome and PBMC transcriptome through GSEA based on Reactome database of curated gene sets. **L** Bubble plot displaying the immune pathways identified in PBMC and muscle transcriptome through GSEA based on hallmark gene sets, including both activated (Red) and suppressed (Blue) pathways

systemic and local immunomodulation. PCA revealed a more distinct variance between muscle samples after exercise compared to PBMC, suggesting that the molecular changes induced by exercise had a more pronounced impact on the muscle tissue (Additional file 1: Fig. S4D, F). However, sPLS-DA still demonstrated a clear variance between the groups in PBMC (Additional file 1: Fig. S4E). In our analysis of the PBMC transcriptome, we identified 90 upregulated DEGs and 66 downregulated DEGs (FC > 1.5, adjusted *P*-value < 0.05). Notably, among the upregulated DEGs, a significant proportion were found to be involved in humoral immunity and complement activation, such as *Cd22*, *Ighg2b*, *Ighg2c*, and *Igha* (Additional file 1: Fig. S4H). Consistent with the findings of mouse plasma proteomics, GO analysis of the upregulated DEGs revealed top enriched pathways primarily associated with humoral immune response (adjusted *P*-value < 0.05), complement activation (adjusted *P*-value < 0.1), and B cell-related immune functions (adjusted *P*-value < 0.1; Additional file 1: Fig. S4I). Thus, we conducted a comprehensive investigation of the immune signaling pathways involved in upregulated DEPs and overall PBMC DEGs through Ingenuity pathway analysis (IPA) platform, and several shared pathways were found, including systemic lupus erythematosus in B cell signaling pathway, IL-7 signaling pathway, FcγRIIB signaling in B lymphocytes, and B cell receptor signaling (Fig. 4J). GSEA further underscored the consistency between the protein and transcript levels, emphasizing the robustness of immune-related pathways in response to resistance exercise. Based on gene sets of canonical pathways, it was also supported that the shared enriched pathways at the protein and transcript levels predominantly revolved the pathways of complement activation and B cell receptor signaling, as well as the activation of NF-κB pathway (Fig. 4K). Additionally, GSEA of PBMC transcriptome based on ontology gene sets confirmed the activation of molecular mediator production in immune response, particularly immunoglobulin synthesis (Additional file 1: Fig. S4J). The analysis also revealed the activation of other key immune processes, such as the interleukin-17 signaling pathway and CD40 signaling pathway (Additional file 1: Fig. S4J). Of note, it was revealed significant suppression of the biological functions associated with various myeloid cells (Additional file 1: Fig. S4k). In line with the previous reports [43], it was also noted the suppression of the interferon signaling pathway in both PBMC and muscle tissue, which supported the consistency between the local immune microenvironment within muscle tissue and the systemic immune environment represented by PBMC in response to resistance exercise (Fig. 4L). Alongside the finding of the immune response induced by resistance exercise, an intriguing discovery that the enhancement of the signaling pathways associated with neural regeneration systematically and locally was observed, suggesting the potential beneficial effects on neural repair of resistance exercise (Additional file 1: Fig. S4G, L).

Since RNA-seq revealed the modulation of PBMC function in mice following weight-loaded ladder-climbing training, we further assessed peripheral blood using flow cytometry to explore changes in cell composition. The analysis was divided into two panels: lymphoid and myeloid (Additional file 1: Fig. S5A-D). Interestingly, while RNA-seq indicated significant alterations in B cell functionality, the proportion of B cells in mice significantly decreased after 4 weeks of resistance training (Additional file 1: Fig. S5E). Conversely, there was a trend towards an increase in the proportions of $CD27^+$ memory B cells and plasma cells (Additional file 1: Fig. S5E). This trend aligns with the cell proportions calculated from the deconvolution of RNA-seq data in SCI patients (Additional file 1: Fig. S3H-J). In contrast, the proportion of T cells in mice significantly increased; however, the proportions of $CD4^+$ and $CD8^+$ T cells remained largely unchanged. Notably, the percentage of $CD25^+$ regulatory T cells (Tregs) significantly increased, accompanied by a rise in activated T cells (Additional file 1: Fig. S5E). Similar trends were observed in human data, showing an increase in Tregs. However, unlike the mouse model, patients in the isotonic exercise treatment group exhibited a significant increase in the proportion of $CD8^+$ T cells. In the myeloid panel, both neutrophils and macrophages displayed varying degrees of decrease (Additional file 1: Fig. S5E). Collectively, these findings suggest that the regulation of peripheral immune cells by resistance exercise exhibits both conservation and species specificity, highlighting the need for further investigation into the changes in cell subpopulations. Importantly, the mice subjected to weight-loaded ladder-climbing demonstrated immune responses that were analogous to those observed in incomplete SCI patients, thereby reinforcing the findings obtained from our human experiments.

Resistance exercise improves lipid metabolism in mice

Since changes in metabolites are a crucial aspect of the physiological response to exercise [44, 45], we conducted a comprehensive analysis to investigate alterations in the plasma metabolome following resistance exercise. A total of 923 metabolites were annotated by LC–MS analysis, the majority of which were lipids and amino acids, and their derivatives (Additional file 1: Fig. S6A). Three-dimensional PCA revealed noticeable differences in variance between the plasma metabolomes of mice following exercise compared to those in the sedentary condition (Fig. 5A). The CV within the two groups were

found to be similar, indicating the stability and comparability of the data (Fig. 5B). Orthogonal projections to latent structures discriminant analysis (OPLS-DA) ($R^2Y = 0.993$, $Q^2Y = 0.71$) was performed to identify differentially expressed metabolites (DEMs) (Fig. 5C). The accuracy and predictive capacity of the model were confirmed through permutation tests (Additional file 1: Fig. S6B). Ultimately, we identified 79 significant metabolites [variable importance in projection (VIP) > 1, FC > 1.2, and adjusted *P*-value < 0.2], with 35 upregulated DEMs and 44 downregulated DEMs, the majority of which belonged to the lipid super-pathway (Fig. 5D). Hierarchical clustering analysis revealed distinct expression patterns among these DEMs, and DEMs belonging to the same super-pathway showed similar expression patterns (Fig. 5E). Additionally, IPA of upregulated DEMs highlighted significant enrichment of the metabolic pathways, including triglyceride biosynthesis, aryl hydrocarbon receptor signaling, and glycerophospholipid biosynthesis (Fig. 5F). Notably, GSEA of the proteomic profiling also identified the activation of lipid-related pathways (Additional file 1: Fig. S6C). Furthermore, gene set variation analysis (GSVA) validated the significant enrichment of lipid-related signaling pathways (FC > 1.5, adjusted *P*-value < 0.05) among the upregulated pathways (Additional file 1: Fig. S6D). Through a network analysis of Spearman's rank correlation, we observed similar patterns of alterations among most lipid molecules, indicating their higher centrality within the network (Additional file 1: Fig. S6E). Importantly, within the network of differentially expressed lipids, a set of lysoglycerophospholipids emerged as top-ranked, underscoring their significance in the physiological response to short-term resistance exercise (Additional file 1: Fig. S6F). VIP of all DEMs further demonstrated the prominence of lysoglycerophospholipids in the exercise induced plasma metabolome compared to the sedentary condition (Fig. 5G and Additional file 1: Fig. S6G). Furthermore, we aimed to delve deeper into the relationship between changes in immune function and metabolic alterations induced by resistance exercise. Ultimately, we made a significant discovery of strong correlations between seven metabolites and differential expressed immunoglobulin heavy chains in plasma proteome (IGHG2B, IGHG2C, IGHV5-12, IGHV1-31, and IGHV1-82). These metabolites include 8,15-Dihete, 2-Ethyl-2-hydroxybutyric acid, 3-Hydroxy-4-methoxybenzoic acid, FFA (16:1), PA (18:1(9Z)/18:1(9Z)), S − Allyl − L − cysteine, and LPE(P − 17:0) (Fig. 5H). Notably, five of these metabolites belong to the lipid molecules. Overall, our findings indicated that short-term resistance exercise predominantly induced alterations in lipid metabolism, with a particular emphasis on lysoglycerophospholipids. Furthermore, the interaction between lipid metabolites and immune molecules provided valuable insights into the intricate interplay between lipid metabolism and immune regulation.

Resistance exercise plasma facilitates locomotor functional recovery after spinal cord injury in non-acute phase

Given the strong correlations between the improvement of locomotor function and the exercise induced alterations of systemic immune environment in incomplete SCI patients, as well as the similarity of physiological changes exhibited by mice, we formulated a hypothesis that post-exercise plasma could potentially mimic the therapeutic effects of resistance exercise in facilitating locomotor function after SCI. To test this hypothesis, we established a mouse model of impaired locomotor function following SCI by clip compression (Fig. 6A and Additional file 1: Fig. S7A, B). To mimic the condition of receiving physical rehabilitation treatment more faithfully in humans, our study deliberately targeted the non-acute phase of

(See figure on next page.)

Fig. 5 Plasma metabolomic profiling in response to exercise. **A** Three-dimensional scatter plot showing PCA of plasma metabolomic data in response to exercise. Each dot represents a sample ($n = 8$). **B** Violin plots showing inter-individual variability of metabolomic data in sedentary group (Sed; Blue) and exercise group (Exe; Red). Boxes are median and interquartile range (IQR, 25th–75th percentile). Each dot (Light gray) represents coefficient of variation for each metabolite. **C** Scatter plots presenting orthogonal projections to latent structures discriminant analysis (OPLS-DA) of plasma metabolomic data in response to exercise. Each dot represents a sample ($n = 8$). **D** Scatter plot (S-plot) generated by OPLS-DA. The S-plot visualizes the variable influence within a model, combining covariance and correlation loading profiles derived from a projection-based model. The *x*-axis of the S-plot represents the contribution (covariance), while the *y*-axis ranges from − 1 to + 1, reflecting the correlation (reliability), which has a theoretical minimum of − 1 and a maximum of + 1. Pie diagrams representing the proportion of differentially expressed metabolites (DEMs) in each super-pathway. Each dot represents a metabolite, with dots closer to the top right and bottom left corners contributing the most to the variance of OPLS-DA. Size of the dots represents the fold change relative to the sedentary group in the linear regression model, while colors indicate the classification of the super-pathway. **E** Heatmap showing hierarchical clustering analysis of exercise-responsive DEMs. Colors represent the classification of the super-pathway or sub-pathway. **F** Bar plot showing the enriched pathways based on IPA of the upregulated DEMs. **G** Bar plot presenting variable importance in projection (VIP) scores of differentially expressed lipid molecules generated by OPLS-DA. Red bars represent contributing to exercise group, and blue bars represent contributing to sedentary group. **H** The curve displaying Mantel's test between the selected protein set and DEMs, while the heatmap in the top right corner representing Spearman's rank correlation between DEMs. In the heatmap, colors represent the correlation coefficient, with no color indicating no significant correlation. Colors of the lines represent *P*-value of Mantel's test, while width of the lines represents the correlation coefficient of Mantel's test

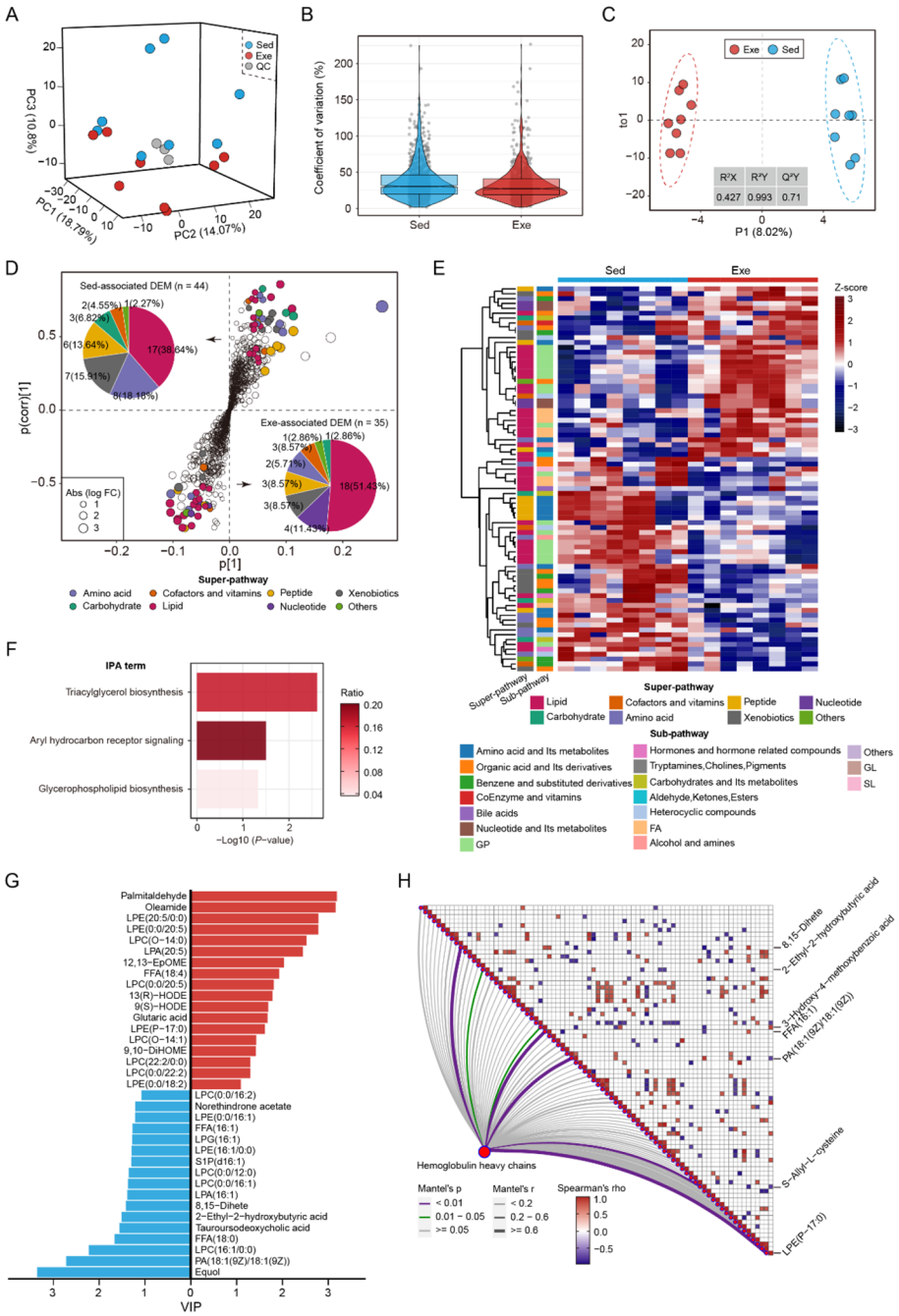

Fig. 5 (See legend on previous page.)

injury, which was also based on the aim of closely simulating the clinical setting where individuals typically commence physical rehabilitation once the acute phase of their injury has subsided. Exercise plasma (EP) obtained from mice accessing weight-loaded ladder-climbing exercise as the intervention group was administered intravenously into the SCI mice from 14 DPI. As a control, sedentary plasma (SP) was collected from mice that did not undergo weight-loaded ladder-climbing exercise. The hindlimb mobility of the mice was evaluated weekly using the Basso Mouse Scale (BMS) score. Indeed, hindlimb mobility in all groups of mice showed a gradual improvement, as indicated by the BMS scores (Fig. 6B). Notably, the mice treated with EP (SCI + EP group) exhibited significantly better performance compared to the control groups starting from 28 DPI, and this superior

performance was maintained over the course of the study (Fig. 6B and Additional file 1: Fig. S7C, D). At 84 DPI, a comprehensive gait analysis was performed to evaluate the effects of treatment on hindlimb motor function in the mice (Fig. 6C). The SCI + EP group exhibited the significant improvements in stance width, stride length, and frequency of toe dragging compared to the SCI + SP group and SCI group, suggesting that the administration of EP had a positive impact on restoring normal gait patterns following SCI (Fig. 6D–F). Additionally, an inclined plane test was conducted to assess hindlimb support and balance ability. Remarkably, the SCI + EP group demonstrated superior recovery compared to both the SCI + SP group and the SCI group as well (Fig. 6G). Furthermore, the histopathological morphology of the spinal cord tissue was analyzed. The hematoxylin and eosin (HE) and Luxol fast blue (LFB) staining revealed extensive demyelination and vacuolization in the lesion area of the spinal cord following SCI (Fig. 6H). Mice treated with SP did not show significant improvement, while mice treated with EP exhibited reduced vacuolization and enhanced preservation of myelin sheaths (Fig. 6I). Nissl staining revealed a noteworthy decrease in the number and staining intensity of Nissl bodies in the anterior horn of the spinal cord following injury; however, mice receiving EP treatment showed a significant recovery in the number of Nissl bodies compared to the control groups (Fig. 6J, K), indicating that the infusion of EP mitigated apoptosis of motor neurons in the anterior horn. Based on our previous findings, both plasma factors and PBMC functions exhibited changes following resistance exercise in mice. Consequently, in addition to administering plasma for treatment, we also administered intravenously post-exercise PBMC to the SCI mice. However, contrary to our expectations, the post-exercise PBMC dosage and treatment regimen employed did not effectively improve locomotor function following SCI when compared to the administration of sedentary PBMC (Additional file 1: Fig. S8A-D). Furthermore, pathological analysis of the injured spinal cord indicated that treatment with post-exercise PBMC did not significantly ameliorate the demyelination or neuronal damage observed (Additional file 1: Fig. S8E-H). Collectively, it was demonstrated that the resistance exercise plasma directly conferred neuroprotection via reduction of demyelination and inhibition of neuronal apoptosis, which holds promise as a potential therapeutic approach to promote the recovery of locomotor function following SCI.

Discussion

Currently, much attention has been given to the physiological responses to acute exercise, as most substances involved in these responses return to resting levels shortly after exercise cessation [46]. Our research aimed to shift the focus towards investigating a physiological state that could be maintained consistently following resistance exercise. Subsequent investigations from our research have demonstrated that plasma molecules stably induced by resistance exercise possess the capability to directly exert neuroprotective effects via mitigating demyelination and inhibiting neuronal apoptosis, ultimately facilitating the recovery of motor function following SCI. Although the specific key molecules responsible for these neuroprotective effects have not yet been identified, we provide the evidence that these effects are supposed be associated with the complement pathways and humoral immune response. Thus, further research should focus on investigating the specific immune-modulatory molecules that play pivotal roles in neuroprotection.

Indeed, considerable evidence from a set of clinical trials supports the effectiveness of long-term resistance training (typically 12 weeks) in enhancing muscle

(See figure on next page.)

Fig. 6 Exercise plasma improves neurological outcomes and locomotor functional recovery following SCI in non-acute phase. **A** Overview of mice experimental strategy. Plasma was administered via tail vein injection from 14 days post injury. The injection strategy consisted of 8 injections over 24 days. Subsequently, behavioral tests were conducted, followed by histopathological examination of the lesioned tissue (Created with BioRender). **B** Basso Mouse Scale (BMS) scores were evaluated in an open field at different time-points (0, 14, 21, 28, 35, 42, 56, 70, and 84 days post injury). Two-way repeated-measures ANOVA with Tukey's multiple comparisons test, $n = 5$–12. $^{*}P < 0.05$, SCI + EP versus SC. **C** Representative images of footprints used to analyze recovery of hindlimb motor function at 84 days post injury. The forelimb footprints are shown in blue, and the hindlimb footprints in red. **D–F** Statistical results of the footprint analysis, including stance width (**D**), stride length (**E**), and toe dragging (**F**), at 84 days post injury. Data are expressed as means ± SEM. One-way ANOVA with Tukey's multiple comparisons test, $n = 5$. $^{*}P < 0.05$, $^{**}P < 0.01$, and $^{***}P < 0.001$. **G** Statistical results of inclined plate test at 84 days post injury. Data are expressed as means ± SEM. One-way ANOVA with Tukey's multiple comparisons test, $n = 5$–12. $^{*}P < 0.05$, $^{**}P < 0.01$, $^{***}P < 0.001$, and $^{****}P < 0.0001$. **H** Representative images showing HE and LFB staining of the transverse spinal cord sections at 84 days post injury. Scale bars: 200, 200, and 50 μm. **I** Statistical results of demyelination according to LFB staining. Data are expressed as means ± SEM. One-way ANOVA with Tukey's multiple comparisons test, $n = 3$–6. $^{*}P < 0.05$, $^{**}P < 0.01$, $^{***}P < 0.001$, and $^{****}P < 0.0001$. **J** Representative images showing Nissl staining of the transverse spinal cord sections at 84 days post injury. The arrows indicate Nissl bodies. Scale bars: 100 μm. **K** Statistical results of neuron survival in anterior horn according to Nissl staining. Statistical method: in each biological sample, two fields of view were selected on both the left and right sides of the spinal anterior horn (×40 objective, with an area size of 640 × 365 μm). Data are expressed as means ± SEM. One-way ANOVA with Tukey's multiple comparisons test, $n = 6$–10 fields. $^{*}P < 0.05$, $^{**}P < 0.01$, $^{***}P < 0.001$, and $^{****}P < 0.0001$

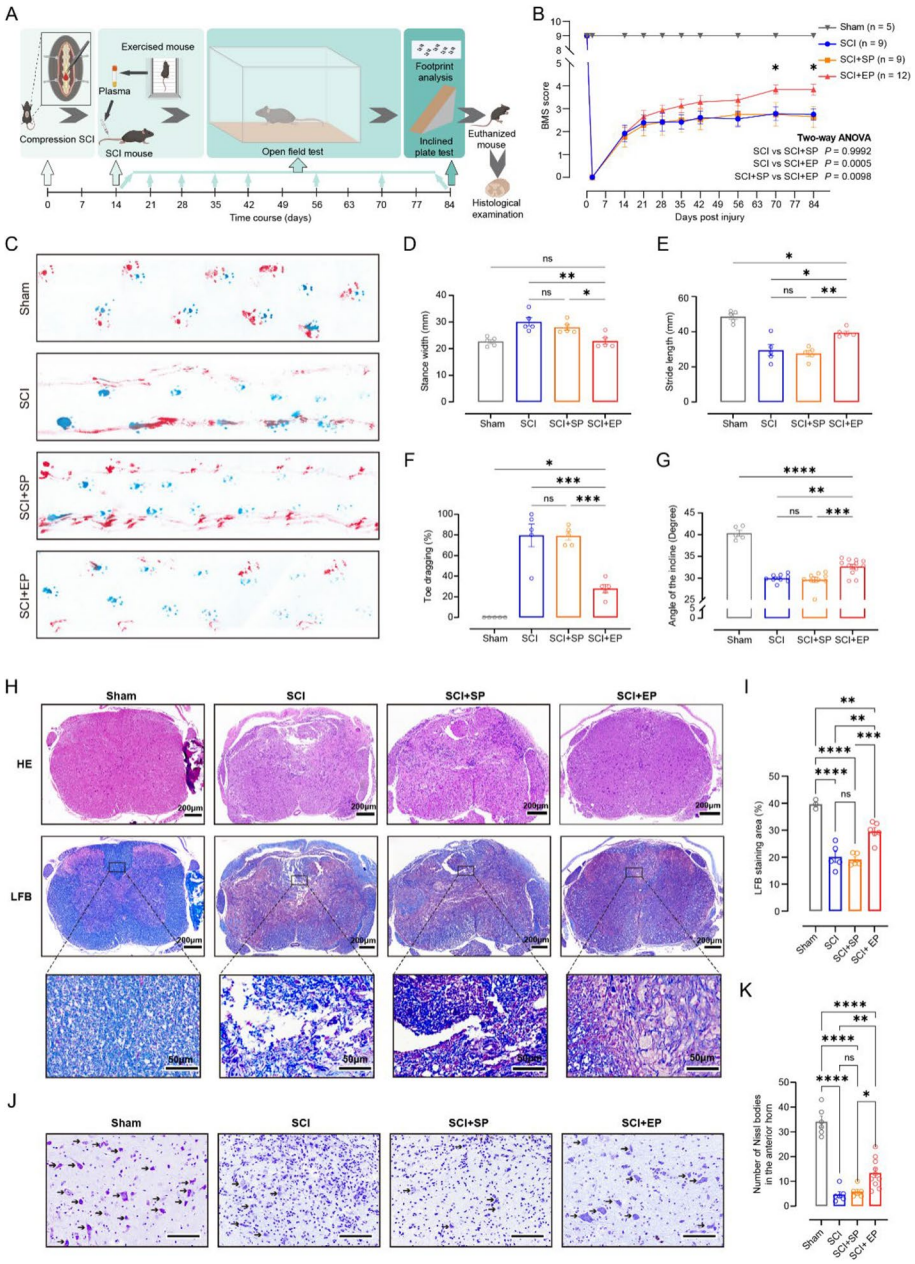

Fig. 6 (See legend on previous page.)

strength in partially paralyzed muscles following SCI [26, 47]. In our study, it was observed significant improvements in muscle strength even with a shortened duration of resistance exercise training (4 weeks). Consistent with the previous studies investigating the effects of long-term training [48, 49], the significant improvements of in all the locomotor-related clinical outcomes provide consistent evidence of the effectiveness of the short-term resistance exercise intervention on enhancing lower limb locomotor function. Notably, the finding that changes in targeted muscular strength did not demonstrate strong correlations with improvements in the locomotor functional outcomes supports our hypothesis that enhanced muscle strength does not exclusively drive the recovery of mobility in SCI patients, prompting us to further analyze systematic molecular changes. In subgroup analysis, it was demonstrated that isotonic exercise training yielded superior effects on improving the ambulatory capacity compared to isometric exercise training, which would also be attributed to its ability to more effectively induce plasma molecular changes related to the complement pathways and humoral immune response.

Researchers became aware of the impact of exercise on the immune system decades ago [50, 51]. In human studies, the effects of chronic exercise on the immune system are contingent upon exercise intensity. Moderate exercise has been associated with immune enhancement, whereas high-intensity or even exhausting exercise may potentially lead to immune suppression [4]. Importantly, the complement system, a crucial element of the innate immune system, is known to be influenced by exercise [52]. Previous studies have suggested that the complement system is susceptible to activation during acute exercise [53]. However, in the context of chronic exercise, its response is comparatively weaker and exhibits heterogeneity, likely influenced by variations in training methods and duration. To illustrate, a study involving a 4-week resistance exercise intervention in well-trained young men demonstrated no alterations in resting C1 or C3 family proteins in the blood [54]. Conversely, in an intervention that spanned 12 weeks and focused on progressive resistance training in older adults, reduced levels of C1q were observed, which corresponded to increased muscle cross-sectional area [55]. Our results demonstrated significant downregulation of C1QB and C1QA, as well as upregulation of C8A following 4 weeks of resistance exercise. In contrast, the scenario differed in mice, as no significant changes were observed in C1, C2, C3, or C8 proteins following resistance exercise, which reveals the inconsistency between studies in animals and humans. This discrepancy is also evident in the transcriptome analysis, where resistance training was found to inhibit the function of human B lymphocytes while in mice, it was observed to enhance B lymphocytes function. Collectively, exercise-induced physiological responses exhibit considerable variability depending on the specific mode, intensity, and duration of exercise. Furthermore, factors such as the sampling time of exercise exposure, as well as the individual's physiological state, can exert notable influences on the outcomes observed [56]. Our study seeks to elucidate the physiological response to resistance exercise in individuals with SCI, utilizing a multi-omics molecular approach. Given the limited body of previous research in this specific population, it is imperative that our results are followed up with additional experimental validations to confirm and extend our findings.

As the limited regenerative capacity of neurons, repair of damage to the central nervous system remains formidable challenges [57]. Previous research has provided evidence that exercise-induced molecules in blood possess the capacity to directly transmit neuroprotective effects, suppressing inflammation [22] and facilitating neurogenesis [23], which are involved in the complement coagulation pathway. Our comprehensive multi-omics analysis has unveiled that substances present in the plasma following resistance exercise also possess the capability to directly confer neuroprotective effects in SCI, most critical of which should be the immunomodulatory molecules of humoral immunity. Intriguingly, although notable changes were observed in PBMC of mice following resistance exercise, these alterations did not yield sufficient therapeutic effects. We propose that the narrow therapeutic window for PBMC treatment may require specific injury levels and timely administration to achieve optimal efficacy. Our research indicates that B cells undergo significant functional changes following resistance exercise. Previous studies have shown that specific subpopulations of B cells possess the potential to repair tissue damage, demonstrating considerable therapeutic efficacy when enriched B cells are administered [58]. Thus, a low abundance of effector cells may also contribute to the limited effectiveness of PBMC treatment. We also postulate that upon transplantation into recipients, these B lymphocytes may exhibit inadequate production of immune regulatory molecules, thus limiting their capacity for optimal therapeutic efficacy. Therefore, future investigations should concentrate on the functional alterations of specific cell subpopulations while also exploring optimal dosage and duration for cell therapy. Indeed, immunoglobulins, secreted by B cells, serve as key representatives of humoral immunomodulatory factors. Numerous studies have highlighted the role of immunoglobulins in suppressing inflammation in the treatment of SCI [59–61]. These findings align with the focus and direction of our research endeavors.

However, it is important to acknowledge the limitations of our study. Firstly, the sample size in the clinical trials was small. Our multi-omics data analysis reveals substantial heterogeneity among patients. Consequently, increasing the sample size can effectively mitigate biases arising from this heterogeneity, thereby enhancing statistical power. Although our cohort of patients included a similar number to previous studies [47, 62], we encountered challenges in obtaining sufficient blood samples for multiple omics analyses due to patient refusal or improper sample storage, which may constrain the detection of subtle differences in the research. Notably, a crossover trial design can substantially increase the sample size and effectively reduce heterogeneity between different groups, which has been employed in many small-sample clinical studies related to exercise interventions [63, 64]. While it remains uncertain whether a crossover design will yield persistent effects on tissue, it is nonetheless a method worth considering for small sample studies. Another limitation is the absence of a parallel control group consisting of incomplete SCI patients without receiving resistance rehabilitation therapy. While two types

of resistance training with different activity levels were included as a form of mutual control, the addition of a dedicated control group would have provided valuable insights. The inclusion of a control group that did not undergo exercise would have helped control for spontaneous changes in plasma molecules. Nevertheless, our findings from subsequent animal experiments have corroborated similar physiological responses observed in humans, further strengthening the credibility of our study. The third limitation is that we utilized a single-sex mouse model for the establishment of the resistance exercise protocol. In reality, the participant cohort includes both males and females; however, during our animal experiments, we exclusively employed male mice for the weight-loaded ladder-climbing experiment. This choice might have diminished the generalizability of our findings. Therefore, the optimal design for our plasma transfer experiment should involve the simultaneous training of both male and female mice to compare the differences in plasma molecular changes between sexes, as well as the differences in therapeutic effects of plasma derived from different sexes.

Conclusions

Taken together, our study has provided comprehensive evidence of the physiological responses to resistance exercise in individuals with incomplete SCI. The results highlight that resistance exercise can effectively modulate the complement pathway and humoral immunity in SCI patients, potentially serving as key factors in promoting the recovery of locomotor function. Furthermore, our findings have been reinforced by subsequent animal experiments involving the administration of exercise plasma, which have demonstrated its direct neuroprotective effects. These findings pave the way for further exploration of exercise mimetics as potential therapeutic strategies for individuals with SCI.

Supplementary information.

Supplementary Information

The online version contains supplementary material available at https://doi.org/10.1186/s13073-025-01434-8.

Additional file 1: Fig. S1. The mutual relationships of clinical outcomes, and the ultimate impact of resistance exercise on clinical outcomes. Fig. S2. Quality controls and analysis for proteomic data in human. Fig. S3. Changes in the PBMC transcriptome in response to resistance exercise in human. Fig. S4. Functional enrichment analyses in response to exercise in mice. Fig. S5. Immune cells in response to exercise in mice. Fig. S6. Resistance exercise-induced lipid metabolism in mice. Fig. S7. Exercise plasma treating locomotor disability following SCI. Fig. S8. Exercise-derived PBMC intravenous infusion in SCI mice with paralysis.

Additional file 2: Fig. S1. CONSORT diagram. Table. S1. Characteristics of the participants ultimately included in the study.

Additional file 3: Study protocol.

Acknowledgements

We extend our gratitude to all participants and their families for their support of this study. We thank the Proteomics Platform of Core Facility of Basic Medical Sciences, Shanghai Jiao Tong University School of Medicine (SJTU-SM) for assistance of proteomics analysis and Wuhan Metware Biotechnology Co., Ltd. for assistance of metabolomics analysis.

Authors' contributions

L.C., Y.F., H.L., R.Z., and J.C. conceived the project, developed methodologies, analyzed data, and wrote the manuscript. J.C., J.Y., and Z.O. performed the clinical trial, collected human samples, and helped analyze the data. R.Z., Y.T., X.D., L.Z., S.X., and L.D. performed animal experiments, collected mice samples, conducted cellular and molecular experiments, and reviewed the manuscript. R.Z., P.Y., C.W., J.Q., and T.Y. performed statistical and bioinformatic analyses. L.C. and Y.F. supervised the project, provided guidance and mentorship to the team, and edited the manuscript. All authors have read and agreed to the content of the manuscript.

Funding

This work is supported by the Shanghai Municipal Health Commission (2022XD050), the Shanghai Municipal Education Commission (22SG12), the National Key R&D Program of China (2024YFA1803503, 2023YFC2508900), the Shanghai YangZhi Rehabilitation Hospital (Shanghai Sunshine Rehabilitation Center) (KYPY202009), the Research Project of China Disabled Person's Federation—on assistive technology (2023CDPFAT-30), the Rehabilitation Policy Research Project of Shanghai Disabled Persons' Federation (2023 ZC1014), the Talent Cultivation Plan of Shanghai YangZhi Rehabilitation Hospital (Shanghai Sunshine Rehabilitation Center) (2022GGRC06), the National clinical key specialty construction project of China (Z155080000004), the Shanghai Research Center of Rehabilitation Medicine (Top Priority Research Center of Shanghai) (2023ZZ02027), the Shanghai Clinical Research Ward (SHDC2023CRW018B), the Shanghai Disabled Persons' Federation Key Laboratory of Intelligent Rehabilitation Assistive Appliance and Technology, and the Shanghai Hospital Development Center Foundation-Shanghai Municipal Hospital Rehabilitation Medicine Specialty Alliance (SHDC22023304).

Data availability

The human original RNA sequence data reported in this paper have been deposited in the Genome Sequence Archive for Human (GSA-Human) repository under the identifier (HRA010133) https://ngdc.cncb.ac.cn/gsa-human/browse/HRA010133 [65]. The mouse original RNA sequence data have been deposited in the GSA repository under the identifier (CRA022293) (https://ngdc.cncb.ac.cn/gsa/browse/CRA022293) [66].
The proteomics and metabolomics data reported in this paper have been deposited in the OMIX repository, China National Center for Bioinformation/Beijing Institute of Genomics under the identifiers (OMIX008713) (https://ngdc.cncb.ac.cn/omix/release/OMIX008713) [67], (OMIX008705) (https://ngdc.cncb.ac.cn/omix/release/OMIX008705) [68], and (OMIX008738) (https://ngdc.cncb.ac.cn/omix/release/OMIX008738) [69]. The mass spectrometry proteomics data have also been deposited to the ProteomeXchange Consortium via the iProX partner repository with the dataset identifier PXD060193 (http://proteomecentral.proteomexchange.org/cgi/GetDataset?ID=PXD060193) [70] and PXD060217 (http://proteomecentral.proteomexchange.org/cgi/GetDataset?ID=PXD060217) [71].

Declarations

Ethics approval and consent to participate

This human trial was approved by the Ethics Committee of the Shanghai Yangzhi Rehabilitation Hospital (YZ-2020–019). The study was carried out in accordance with The Code of Ethics of the World Medical Association (Declaration of Helsinki) for experiments involving humans. All the participants signed the informed consent form to participate and for use of their tissue for research before the trial. The animal study was carried out in compliance with the Animal Research: Reporting of In Vivo Experiments guidelines and the ARRIVE guidelines, as overseen by the Institutional Animal Care and Use Committee of youshulife Co. (YS-m202212001).

Consent for publication

Not applicable.

Competing interests
The authors declare that they have no competing interests.

Author details
[1]Shanghai Institute of Hematology, State Key Laboratory of Medical Genomics, National Research Center for Translational Medicine at Shanghai, Ruijin Hospital, Shanghai Jiao Tong University School of Medicine, Shanghai 200025, China. [2]Department of Neurology and Neurological Rehabilitation, Shanghai YangZhi Rehabilitation Hospital (Shanghai Sunshine Rehabilitation Center), Tongji University School of Medicine, Shanghai 201619, China. [3]Department of General Medicine, Ruijin Hospital, Shanghai Jiaotong University School of Medicine, Shanghai 200025, China. [4]Department of Emergency, Ruijin Hospital, Shanghai Jiaotong University School of Medicine, Shanghai 200025, China. [5]Department of Cardiac Surgery, Ruijin Hospital, Shanghai Jiaotong University School of Medicine, Shanghai 200025, China.

Received: 11 April 2024 Accepted: 24 January 2025
Published online: 05 February 2025

References

1. Gulsin GS, Henson J, Brady EM, Sargeant JA, Wilmot EG, Athithan L, et al. Cardiovascular determinants of aerobic exercise capacity in adults with type 2 diabetes. Diabetes Care. 2020;43:2248–56.
2. Hagar A, Wang Z, Koyama S, Serrano JA, Melo L, Vargas S, et al. Endurance training slows breast tumor growth in mice by suppressing Treg cells recruitment to tumors. BMC Cancer. 2019;19:536.
3. Zhang H, Chen T, Ren J, Xia Y, Onuma A, Wang Y, et al. Pre-operative exercise therapy triggers anti-inflammatory trained immunity of kupffer cells through metabolic reprogramming. Nat Metab. 2021;3:843–58.
4. Chow LS, Gerszten RE, Taylor JM, Pedersen BK, van Praag H, Trappe S, et al. Exerkines in health, resilience and disease. Nat Rev Endocrinol. 2022;18:273–89.
5. Chen J, Zhou R, Feng Y, Cheng L. Molecular mechanisms of exercise contributing to tissue regeneration. Signal Transduct Target Ther. 2022;7:383.
6. Gubert C, Hannan AJ. Exercise mimetics: Harnessing the therapeutic effects of physical activity. Nat Rev Drug Discov. 2021;20:862–79.
7. Augusto-Oliveira M, Arrifano GP, Leal-Nazare CG, Santos-Sacramento L, Lopes-Araujo A, Royes LFF, et al. Exercise reshapes the brain: Molecular, cellular, and structural changes associated with cognitive improvements. Mol Neurobiol. 2023;60:6950–74.
8. Mak MK, Wong-Yu IS, Shen X, Chung CL. Long-term effects of exercise and physical therapy in people with Parkinson disease. Nat Rev Neurol. 2017;13:689–703.
9. Hornby TG, Reisman DS, Ward IG, Scheets PL, Miller A, Haddad D, et al. Clinical practice guideline to improve locomotor function following chronic stroke, incomplete spinal cord injury, and brain injury. J Neurol Phys Ther. 2020;44:49–100.
10. Martin Ginis KA, van der Scheer JW, Latimer-Cheung AE, Barrow A, Bourne C, Carruthers P, et al. Evidence-based scientific exercise guidelines for adults with spinal cord injury: An update and a new guideline. Spinal Cord. 2018;56:308–21.
11. Gaspar R, Padula N, Freitas TB, de Oliveira JPJ, Torriani-Pasin C. Physical exercise for individuals with spinal cord injury: Systematic review based on the international classification of functioning, disability, and health. J Sport Rehabil. 2019;28:505–16.
12. GBD 2016 Traumatic Brain Injury and Spinal Cord Injury Collaborators. Global, regional, and national burden of traumatic brain injury and spinal cord injury, 1990–2016: A systematic analysis for the global burden of disease study 2016. Lancet Neurol. 2019;18:56–87.
13. Pelletier C. Exercise prescription for persons with spinal cord injury: A review of physiological considerations and evidence-based guidelines. Appl Physiol Nutr Metab. 2023;48:882–95.
14. Sandrow-Feinberg HR, Houle JD. Exercise after spinal cord injury as an agent for neuroprotection, regeneration and rehabilitation. Brain Res. 2015;1619:12–21.
15. Duan R, Qu M, Yuan Y, Lin M, Liu T, Huang W, et al. Clinical benefit of rehabilitation training in spinal cord injury: A systematic review and meta-analysis. Spine (Phila Pa 1976). 2021;46:E398–410.
16. Hicks AL. Locomotor training in people with spinal cord injury: Is this exercise? Spinal Cord. 2021;59:9–16.
17. Shabanzadeh AP, D'Onofrio PM, Magharious M, Choi KAB, Monnier PP, Koeberle PD. Modifying PTEN recruitment promotes neuron survival, regeneration, and functional recovery after CNS injury. Cell Death Dis. 2019;10:567.
18. Hu J, Liu PL, Hua Y, Gao BY, Wang YY, Bai YL, et al. Constraint-induced movement therapy enhances AMPA receptor-dependent synaptic plasticity in the ipsilateral hemisphere following ischemic stroke. Neural Regen Res. 2021;16:319–24.
19. Tang Y, Zhang Y, Zheng M, Chen J, Chen H, Liu N. Effects of treadmill exercise on cerebral angiogenesis and MT1-MMP expression after cerebral ischemia in rats. Brain Behav. 2018;8:e01079.
20. Choi SH, Bylykbashi E, Chatila ZK, Lee SW, Pulli B, Clemenson GD, et al. Combined adult neurogenesis and BDNF mimic exercise effects on cognition in an Alzheimer's mouse model. Science. 2018;361(6406):eaan8821.
21. Ruiz-Gonzalez D, Hernandez-Martinez A, Valenzuela PL, Morales JS, Soriano-Maldonado A. Effects of physical exercise on plasma brain-derived neurotrophic factor in neurodegenerative disorders: A systematic review and meta-analysis of randomized controlled trials. Neurosci Biobehav Rev. 2021;128:394–405.
22. De Miguel Z, Khoury N, Betley MJ, Lehallier B, Willoughby D, Olsson N, et al. Exercise plasma boosts memory and dampens brain inflammation via clusterin. Nature. 2021;600:494–9.
23. Horowitz AM, Fan X, Bieri G, Smith LK, Sanchez-Diaz CI, Schroer AB, et al. Blood factors transfer beneficial effects of exercise on neurogenesis and cognition to the aged brain. Science. 2020;369:167–73.
24. Cohen S, Nathan JA, Goldberg AL. Muscle wasting in disease: Molecular mechanisms and promising therapies. Nat Rev Drug Discov. 2015;14:58–74.
25. Currier BS, McLeod JC, Banfield L, Beyene J, Welton NJ, D'Souza AC, et al. Resistance training prescription for muscle strength and hypertrophy in healthy adults: A systematic review and Bayesian network meta-analysis. Br J Sports Med. 2023;57:1211–20.
26. Santos LV, Pereira ET, Reguera-Garcia MM, Oliveira CEP, Moreira OC. Resistance training and muscle strength in people with spinal cord injury: A systematic review and meta-analysis. J Bodyw Mov Ther. 2022;29:154–60.
27. Rupp R, Biering-Sorensen F, Burns SP, Graves DE, Guest J, Jones L, et al. International standards for neurological classification of spinal cord injury: Revised 2019. Top Spinal Cord Inj Rehabil. 2021;27:1–22.
28. Hornby TG, Lewek MD, Thompson CK, Heitz R. Repeated maximal volitional effort contractions in human spinal cord injury: Initial torque increases and reduced fatigue. Neurorehabil Neural Repair. 2009;23:928–38.
29. Jayaraman A, Thompson CK, Rymer WZ, Hornby TG. Short-term maximal-intensity resistance training increases volitional function and strength in chronic incomplete spinal cord injury: A pilot study. J Neurol Phys Ther. 2013;37:112–7.
30. Bowers EJ, Morgan DL, Proske U. Damage to the human quadriceps muscle from eccentric exercise and the training effect. J Sports Sci. 2004;22:1005–14.
31. Yuan Y, Xu P, Jiang Q, Cai X, Wang T, Peng W, et al. Exercise-induced alpha-ketoglutaric acid stimulates muscle hypertrophy and fat loss through OXGR1-dependent adrenal activation. EMBO J. 2020;39:e103304.
32. Pereira RM, Rodrigues K, Anaruma CP, Sant'Ana MR, de Campos TDP, Gaspar RS, et al. Short-term strength training reduces gluconeogenesis and NAFLD in obese mice. J Endocrinol. 2019;241:59–70.
33. Basso DM, Fisher LC, Anderson AJ, Jakeman LB, McTigue DM, Popovich PG. Basso Mouse Scale for locomotion detects differences in recovery after spinal cord injury in five common mouse strains. J Neurotrauma. 2006;23:635–59.
34. Wells JE, Hurlbert RJ, Fehlings MG, Yong VW. Neuroprotection by minocycline facilitates significant recovery from spinal cord injury in mice. Brain. 2003;126:1628–37.
35. Fan L, Liu C, Chen X, Zheng L, Zou Y, Wen H, et al. Exosomes-loaded electroconductive hydrogel synergistically promotes tissue repair after spinal cord injury via immunoregulation and enhancement of myelinated axon growth. Adv Sci (Weinh). 2022;9:e2105586.
36. Prakash A, Peterman S, Ahmad S, Sarracino D, Frewen B, Vogelsang M, et al. Hybrid data acquisition and processing strategies with increased throughput and selectivity: pSMART analysis for global qualitative and quantitative analysis. J Proteome Res. 2014;13:5415–30.

37. Newman AM, Liu CL, Green MR, Gentles AJ, Feng W, Xu Y, et al. Robust enumeration of cell subsets from tissue expression profiles. Nat Methods. 2015;12:453–7.
38. Ross M, Kargl CK, Ferguson R, Gavin TP, Hellsten Y. Exercise-induced skeletal muscle angiogenesis: Impact of age, sex, angiocrines and cellular mediators. Eur J Appl Physiol. 2023;123:1415–32.
39. Spaulding HR, Yan Z. Ampk and the adaptation to exercise. Annu Rev Physiol. 2022;84:209–27.
40. Sinzinger H, Virgolini I. Effects of exercise on parameters of blood coagulation, platelet function and the prostaglandin system. Sports Med. 1988;6:238–45.
41. Heber S, Volf I. Effects of physical (in)activity on platelet function. Biomed Res Int. 2015;2015:165078.
42. Lundberg Slingsby MH, Nyberg M, Egelund J, Mandrup CM, Frikke-Schmidt R, Kirkby NS, et al. Aerobic exercise training lowers platelet reactivity and improves platelet sensitivity to prostacyclin in pre- and postmenopausal women. J Thromb Haemost. 2017;15:2419–31.
43. Langston PK, Sun Y, Ryback BA, Mueller AL, Spiegelman BM, Benoist C, et al. Regulatory T cells shield muscle mitochondria from interferon-gamma-mediated damage to promote the beneficial effects of exercise. Sci Immunol. 2023;8:eadi5377.
44. Khoramipour K, Sandbakk O, Keshteli AH, Gaeini AA, Wishart DS, Chamari K. Metabolomics in exercise and sports: A systematic review. Sports Med. 2022;52:547–83.
45. Schranner D, Kastenmuller G, Schonfelder M, Romisch-Margl W, Wackerhage H. Metabolite concentration changes in humans after a bout of exercise: A systematic review of exercise metabolomics studies. Sports Med Open. 2020;6:11.
46. Contrepois K, Wu S, Moneghetti KJ, Hornburg D, Ahadi S, Tsai MS, et al. Molecular choreography of acute exercise. Cell. 2020;181(1112–1130):e1116.
47. Aravind N, Harvey LA, Glinsky JV. Physiotherapy interventions for increasing muscle strength in people with spinal cord injuries: A systematic review. Spinal Cord. 2019;57:449–60.
48. Stone WJ, Stevens SL, Fuller DK, Caputo JL. Ambulation and physical function after eccentric resistance training in adults with incomplete spinal cord injury: A feasibility study. J Spinal Cord Med. 2019;42:526–33.
49. Stone WJ, Stevens SL, Fuller DK, Caputo JL. Strength and step activity after eccentric resistance training in those with incomplete spinal cord injuries. Top Spinal Cord Inj Rehabil. 2018;24:343–52.
50. Pedersen BK, Hoffman-Goetz L. Exercise and the immune system: Regulation, integration, and adaptation. Physiol Rev. 2000;80:1055–81.
51. Pedersen BK, Toft AD. Effects of exercise on lymphocytes and cytokines. Br J Sports Med. 2000;34:246–51.
52. Rothschild-Rodriguez D, Causer AJ, Brown FF, Collier-Bain HD, Moore S, Murray J, et al. The effects of exercise on complement system proteins in humans: A systematic scoping review. Exerc Immunol Rev. 2022;28:1–35.
53. Zhang C, Wang C, Li Y, Miwa T, Liu C, Cui W, et al. Complement C3a signaling facilitates skeletal muscle regeneration by regulating monocyte function and trafficking. Nat Commun. 2017;8:2078.
54. Risoy BA, Raastad T, Hallen J, Lappegard KT, Baeverfjord K, Kravdal A, et al. Delayed leukocytosis after hard strength and endurance exercise: Aspects of regulatory mechanisms. BMC Physiol. 2003;3:14.
55. Watanabe S, Sato K, Hasegawa N, Kurihara T, Matsutani K, Sanada K, et al. Serum C1q as a novel biomarker of sarcopenia in older adults. FASEB J. 2015;29:1003–10.
56. Sato S, Dyar KA, Treebak JT, Jepsen SL, Ehrlich AM, Ashcroft SP, et al. Atlas of exercise metabolism reveals time-dependent signatures of metabolic homeostasis. Cell Metab. 2022;34(329–345):e328.
57. Karsy M, Hawryluk G. Modern medical management of spinal cord injury. Curr Neurol Neurosci Rep. 2019;19:65.
58. Wang J, Liu S, Meng X, Zhao X, Wang T, Lei Z, et al. Exercise inhibits doxorubicin-induced cardiotoxicity via regulating b cells. Circ Res. 2024;134:550–68.
59. Fehlings MG, Nguyen DH. Immunoglobulin G: A potential treatment to attenuate neuroinflammation following spinal cord injury. J Clin Immunol. 2010;30(Suppl 1):S109-112.
60. Ulndreaj A, Vidal PM, Forgione N, Hong J, Fehlings MG. IgM immunoglobulin influences recovery after cervical spinal cord injury by modulating the IgG autoantibody response. eNeuro. 2021;8(5):ENEURO.0491-19.2021.
61. Chio JCT, Wang J, Surendran V, Li L, Zavvarian MM, Pieczonka K, et al. Delayed administration of high dose human immunoglobulin G enhances recovery after traumatic cervical spinal cord injury by modulation of neuroinflammation and protection of the blood spinal cord barrier. Neurobiol Dis. 2021;148:105187.
62. Bye EA, Harvey LA, Gambhir A, Kataria C, Glinsky JV, Bowden JL, et al. Strength training for partially paralysed muscles in people with recent spinal cord injury: A within-participant randomised controlled trial. Spinal Cord. 2017;55:460–5.
63. Morville T, Sahl RE, Moritz T, Helge JW, Clemmensen C. Plasma metabolome profiling of resistance exercise and endurance exercise in humans. Cell Rep. 2020;33:108554.
64. Savikj M, Stocks B, Sato S, Caidahl K, Krook A, Deshmukh AS, et al. Exercise timing influences multi-tissue metabolome and skeletal muscle proteome profiles in type 2 diabetic patients - a randomized crossover trial. Metabolism. 2022;135:155268.
65. Zhou R, Chen J, Tang Y, Wei C, Yu P, Ding X, et al. Multi-omics uncovers immune-modulatory molecules in plasma contributing to resistance exercise-ameliorated locomotor disability after incomplete spinal cord injury. Genome Sequence Archive for Human (HRA010133). 2025. https://ngdc.cncb.ac.cn/gsa-human/browse/HRA010133 .
66. Zhou R, Chen J, Tang Y, Wei C, Yu P, Ding X, et al. Multi-omics uncovers immune-modulatory molecules in plasma contributing to resistance exercise-ameliorated locomotor disability after incomplete spinal cord injury. Genome Sequence Archive (CRA022293). 2025. https://ngdc.cncb.ac.cn/gsa/browse/CRA022293 .
67. Zhou R, Chen J, Tang Y, Wei C, Yu P, Ding X, et al. Multi-omics uncovers immune-modulatory molecules in plasma contributing to resistance exercise-ameliorated locomotor disability after incomplete spinal cord injury. OMIX (OMIX008713). 2025. https://ngdc.cncb.ac.cn/omix/release/OMIX008713 .
68. Zhou R, Chen J, Tang Y, Wei C, Yu P, Ding X, et al. Multi-omics uncovers immune-modulatory molecules in plasma contributing to resistance exercise-ameliorated locomotor disability after incomplete spinal cord injury. OMIX (OMIX008705). 2025. https://ngdc.cncb.ac.cn/omix/release/OMIX008705 .
69. Zhou R, Chen J, Tang Y, Wei C, Yu P, Ding X, et al. Multi-omics uncovers immune-modulatory molecules in plasma contributing to resistance exercise-ameliorated locomotor disability after incomplete spinal cord injury. OMIX (OMIX008738). 2025. https://ngdc.cncb.ac.cn/omix/release/OMIX008738 .
70. Zhou R, Chen J, Tang Y, Wei C, Yu P, Ding X, et al. Multi-omics uncovers immune-modulatory molecules in plasma contributing to resistance exercise-ameliorated locomotor disability after incomplete spinal cord injury. 2025. ProteomeXchange Consortium (PXD060193).
71. Zhou R, Chen J, Tang Y, Wei C, Yu P, Ding X, et al. Multi-omics uncovers immune-modulatory molecules in plasma contributing to resistance exercise-ameliorated locomotor disability after incomplete spinal cord injury. 2025. ProteomeXchange Consortium (PXD060217).

Publisher's Note